



5-2008

A Study of Asian Dust Events Using Surface, Satellite, and Aircraft Measurements During Intex-B

Rebecca L. Obrecht

Follow this and additional works at: <https://commons.und.edu/theses>



Part of the [Psychology Commons](#)

Recommended Citation

Obrecht, Rebecca L., "A Study of Asian Dust Events Using Surface, Satellite, and Aircraft Measurements During Intex-B" (2008). *Theses and Dissertations*. 920.

<https://commons.und.edu/theses/920>

This Thesis is brought to you for free and open access by the Theses, Dissertations, and Senior Projects at UND Scholarly Commons. It has been accepted for inclusion in Theses and Dissertations by an authorized administrator of UND Scholarly Commons. For more information, please contact zeineb.yousif@library.und.edu.

A STUDY OF ASIAN DUST EVENTS USING SURFACE, SATELLITE, AND
AIRCRAFT MEASUREMENTS DURING INTEX-B

by

Rebecca L. Obrecht
Bachelor of Science, University of Nebraska-Lincoln, 2004

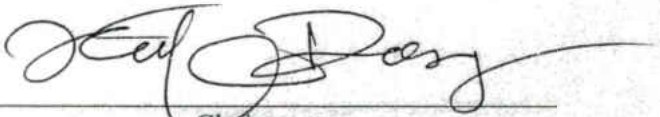
A Thesis
Submitted to the Graduate Faculty
of the
University of North Dakota
in partial fulfillment of the requirements

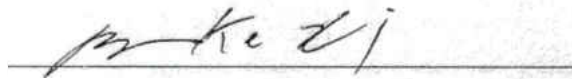
for the degree of
Master of Science

Grand Forks, North Dakota
May
2008

Copyright 2008 Rebecca L. Obrecht

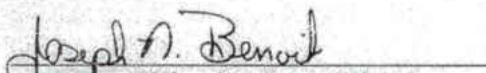
This thesis, submitted by Rebecca L. Obrecht in partial fulfillment of the requirements for the Degree of Master of Science from the University of North Dakota, has been read by the Faculty Advisory Committee under whom the work has been done and is hereby approved.



Chairperson





This thesis meets the standards for appearance, conforms to the style and format requirements of the Graduate School of the University of North Dakota, and is hereby approved.


Dean of the Graduate School


Date

PERMISSION

Title A Study of Asian Dust Events using Surface, Satellite, and Aircraft
Measurements during INTEX-B

Department Atmospheric Sciences

Degree Master of Science

In presenting this thesis in partial fulfillment of the requirements for a graduate degree from the University of North Dakota, I agree that the library of this University shall make it freely available for inspection. I further agree that permission for extensive copying for scholarly purposes may be granted by the professor who supervised my thesis work or, in his absence, by the chairperson of the department or the dean of the Graduate School. It is understood that any copying or publication or other use of this thesis or part thereof for financial gain shall not be allowed without my written permission. It is also understood that due recognition shall be given to me and to the University of North Dakota in any scholarly use which may be made of any material in my thesis.

Signature Rob Gantt

Date April 21, 2008

TABLE OF CONTENTS

LIST OF FIGURES	vii
LIST OF TABLES	x
ACKNOWLEDGEMENTS	xi
ABSTRACT	xii
CHAPTER	
I. INTRODUCTION	1
II. DATA AND METHODOLOGY	8
Surface	8
China	8
North America	12
Satellite	12
UND/NASA DC-8 Aircraft	13
DIAL	13
Nephelometer	14
III. RESULTS	16
Clear-sky (Clean, No Dust)	17
Dust Events	21
Strong Dust Event	22
Weak Dust Event	39
IV. DISCUSSION	53

V. CONCLUSIONS	57
REFERENCES	60

LIST OF FIGURES

Figure		Page
1.	The global mean radiative forcing of the climate system for the year 2000, relative to 1750	2
2.	Map highlighting the extent of the Gobi Desert in northern China and Mongolia	2
3.	The temporal variation of (a) τ_{500} , the optical thickness above 3.6 km altitude and at 500 nm wavelength and (b) back isobaric trajectory at 500 hPa level	5
4.	The Asian dust event of April 1998 as it traveled across the Pacific	5
5.	A map showing all surface sites (Xianghe, China; Trinidad Head, CA; Rimrock, ID; Egbert, ON) used during this study and all ten UND/NASA DC-8 flight tracks during INTEX-B	9
6.	Instruments at the Xianghe, China surface station	11
7.	Schematic of the DIAL system is shown on the left and a picture of the DIAL system on the DC-8 aircraft is shown on the right	15
8.	A time series of (a) insolation, (b) AOD, and Angström exponent over Xianghe, China for the clear-sky event on 10 May 2006	18
9.	AOD (left two images) and TOA albedo (right two images) from Terra (top) and Aqua (bottom) satellites centered over Xianghe, China (white star) during the clear-sky event on 10 May 2006	19
10.	(a) MODIS visible image and (b) mean sea level pressure centered on Xianghe, China during the clear-sky event on 10 May 2006	20
11.	Same as in Figure 10 but for a strong dust event on 17 April 2006	23
12.	Same as in Figure 8 but for a strong dust event on 17 April 2006	24
13.	Same as in Figure 9 but for a strong dust event on 17 April 2006	25

14.	AOD (left) and TOA albedo (right) from Aqua over the Pacific Ocean for 18 April 2006. White star denotes Xianghe, China	27
15.	Same as in Figure 14 but for 19 April 2006	28
16.	Same as in Figure 14 but for 20 April 2006	29
17.	Same as in Figure 14 but for 21 April 2006	30
18.	Same as in Figure 14 but for 22 April 2006	31
19.	Same as in Figure 14 but for 23 April 2006	32
20.	A close-up of the flight track coverage by the DC-8 on 23 April 2006 with MODIS AOD and CERES TOA albedo	33
21.	DC-8 DIAL for 23-24 April 2006 flight	34
22.	DC-8 nephelometer total scattering coefficient profiles at 550 nm for the 23-24 April 2006 flight	36
23.	Forward trajectories as computed by the NOAA HYSPLIT model initialized at Xianghe, China on 17 April 2006 at three altitudes: 3000 m, 5000 m, and 7000 m	38
24.	A time series of (a) AOD and (b) Angstrom exponent at Rimrock, ID from 22-25 April	39
25.	Same as in Figure 10 but for a weak dust event on 7 April 2007	40
26.	Same as in Figure 8 but for a weak dust event on 7 April 2007	41
27.	Same as in Figure 9 but for a weak dust event on 7 May 2006	42
28.	Same as in Figure 14 but for a weak dust event beginning on 7 April 2006	43
29.	Same as in Figure 28 but for 9 April 2006	44
30.	Same as in Figure 28 but for 10 April 2006	45
31.	Same as in Figure 28 but for 17 April 2006	46
32.	Same as in Figure 23 except initialized on 7 April 2006	47
33.	A close-up of the flight track from Figure 36 on 17 April 2006	49

34.	Same as in Figure 21 but for 17-18 April 2006	50
35.	Total scattering coefficients from the nephelometer on the DC-8 on 17 April 2006	51
36.	AOD (a) and AE (b) at Egbert, ON during the period from 13 to 20 April 2006	52

LIST OF TABLES

Table		Page
1.	Summary for the source (Xianghe, China), transport over the Pacific, and sink (North America)	54

ACKNOWLEDGEMENTS

Thank you to my advising committee of Doctors Xiquan Dong, Baike Xi, and George Seielstad for their guidance, expertise, and support. Thank you to all the graduate students in the Atmospheric Sciences Department especially those in my research group (Kathryn Crosby, Zhe Feng, Hongchun Jin, and Aaron Kennedy) for helping me get through this process every step of the way. Thank you to my family and Ian Storey for believing I could do it and for always being there.

This work was supported by the UND National Suborbital Education and Research Center (NSERC) fellowship, directed by Doctors George Seielstad and Rick Shetter. The Xianghe, China EAST-AIRE data were provided by Dr. Zhanqing Li and Maureen Cribb. The AERONET data at Trinidad Head, CA, Rimrock, ID, and Egbert, ON were provided and are maintained by PIs Ellsworth G. Dutton, Brent Holben, and Norm O'Neill, respectively. The UND/NASA DC-8 DIAL (Dr. Edward V. Browell, PI) and nephelometer (Dr. Antony Clarke, PI) data were downloaded from the NASA LaRC INTEX-B website. The CERES SSF data were obtained from the Atmospheric Science Data Center at the NASA Langley Research Center. The HYSPLIT transport model was provided by the NOAA Air Resources Laboratory (ARL) and can be found at the READY website (<http://www.arl.noaa.gov/ready.html>).

ABSTRACT

Asian dust events occur frequently during the northern hemisphere spring season. Some of these events can transport dust downwind to North America within 7 days' time and turn a regional impact into one of a much larger scale. To further quantify the transpacific transport and evolution of Asian dust to North America and assess the impact on regional climate, NASA led a field experiment called the Intercontinental Chemical Transport Experiment – Phase B (INTEX-B) during April-May 2006 over the eastern Pacific Ocean. This study documents the physical and optical properties of Asian dust, as well as its strength and evolution from its source near the Gobi desert to its sink in North America, during INTEX-B using surface, satellite and DC-8 aircraft measurements.

A total of 11 dust events have been identified and summarized. Two dust events, originating from the Gobi desert on 7 and 17 April 2006, have been extensively analyzed, and their trajectories, strength and evolution have been tracked. For the strong Asian dust episode on 17 April 2006, the observed total downwelling shortwave (SW) flux over Xianghe, a site near Beijing, is only 46% of the clear-sky value with almost no direct transmission, and nearly double the diffuse SW clear-sky value. The surface averaged aerosol optical depth (AOD) increased from 0.17 (clear-sky) to 4.0, and the Angström exponent (AE) dropped from 1.26 (clear-sky) to below 0.1. This event was also captured by satellite and the UND/NASA DC-8 over the eastern Pacific Ocean from 23-24 April 2006. By this time, its strength degraded due to dispersion and larger particles settling

out. The DC-8 observed this dust plume with higher averaged aerosol scattering ratios of 10.5 at 1064 nm and 2.0 at 588 nm and a depolarization of 25%. The DC-8 nephelometer also observed this dust event in-situ and confirmed that the highest scattering coefficient ranged from 80-100 mm^{-1} . When this dust transported to North America, its AOD values decreased from a mean of 2.0 over the source region to 0.2 over North America.

CHAPTER I

INTRODUCTION

Dust is a significant type of aerosol that contributes to the aerosol effect and is one of the leading uncertainties in global climate studies today (IPCC 2001, 2007). The Intergovernmental Panel on Climate Change found that mineral dust, under the aerosols heading in Figure 1, may have a net warming or cooling, which is why the level of scientific understanding is very low and needs to be studied.

Dust can have an impact on global/regional climate through its so-called “direct” and “indirect” radiative effects by changing the optical properties of the Earth’s atmosphere through the scattering and absorption of sunlight (Tanré et al. 2001), acting as a suppressant of precipitation (Rosenfeld et al. 2001), and/or contributing to cloud condensation nuclei (Levin and Ganor 1996; DeMott et al. 2003; Huang et al. 2006).

Besides climatic impacts, dust can affect air quality and human health (Prospero 1999). There is some evidence of co-transport of infectious microorganisms that become lofted into the atmosphere along with dust from the Gobi Desert. Influenza-like symptoms have occurred at the Hawaiian Islands after dust plumes linked to Asia have passed (Burdakov and Pole 1984; Tratt et al. 2001). The transport of dust from Asia to North America is also known to cause poor air quality to levels that are associated with adverse health effects, particularly at sites in the western United States (Husar et al. 2001; Jaffe et al. 2003b).

The global mean radiative forcing of the climate system for the year 2000, relative to 1750

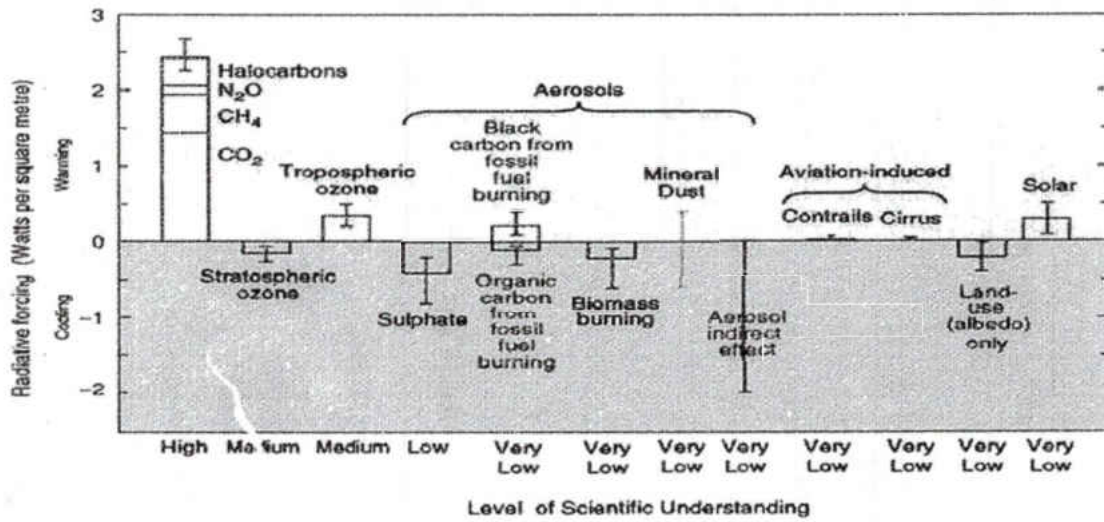


Figure 1. The global mean radiative forcing of the climate system for the year 2000, relative to 1750. (Image from IPCC 2001)

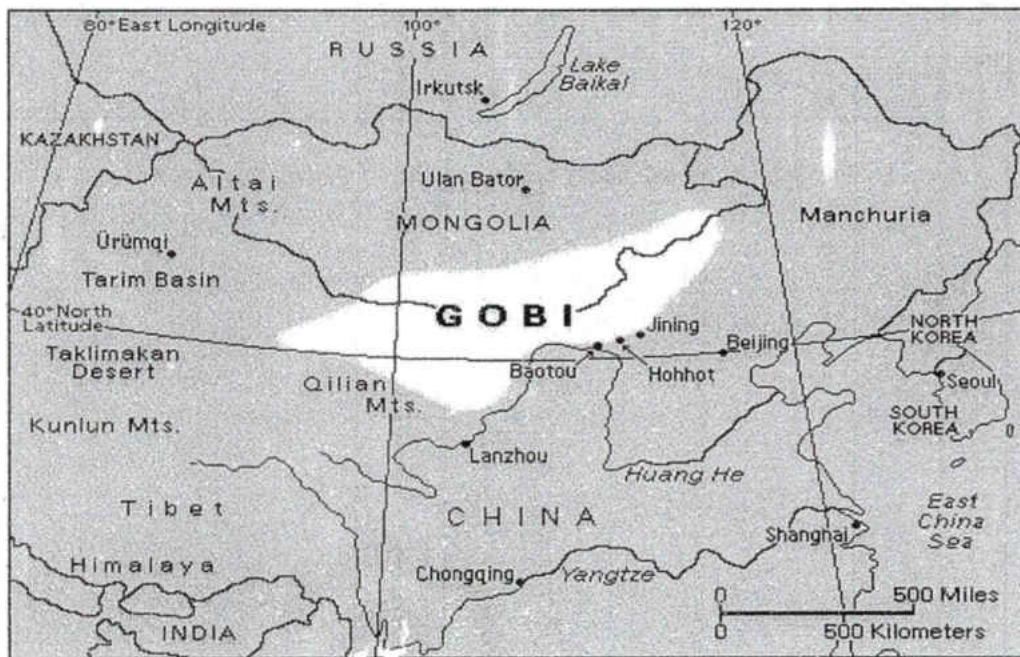


Figure 2. Map highlighting the extent of the Gobi Desert in northern China and Mongolia. (Image from Szykman et al. 2003).

The East Asia region is undergoing rapid population growth and economic/industrial development. Accompanying this development is a rapid increase in energy consumption and emission of atmospheric pollutants. East Asia is also the region where Asian dust episodes occur frequently (Li et al. 2007). Most Asian dust events originate from the Gobi desert between Mongolia and north-central China (Figure 2) under specific meteorological conditions, such as wind speeds greater than 5 m/s associated with a low-pressure system and a dry spring season (Murayama et al. 2001; Husar et al. 2001). Once Asian dust is lifted to the free troposphere and driven by strong westerly winds aloft, these aerosols can travel over long distances, such as from East Asia to North America. Approximately 10% of Asian dust events arrive at the west coast of North America within 7 days, based on 15 years of climatological trajectories (Eckhardt et al. 2004). Therefore, locally produced aerosols with only a regional climatic impact have turned into a large-scale issue after they transport downwind from one continent to another. The process of how these Asian dust properties evolve and impact locations distant from their origin is still in question, and the study of the transcontinental transport of dust and aerosols is an important aspect of understanding their role in regional and global climate change.

Over the past few decades, several field campaigns have been carried out over the western Pacific region to understand the transport of dust from Asia to the Pacific. During the early 1990's (Bachmeier et al. 1996), the Pacific Exploratory Mission (PEM-West A and B) examined the impact of natural and human activities on the troposphere over the northwestern Pacific Ocean. The Aerosol Characterization Experiment-Asia (ACE-Asia) (Huebert et al. 2003), along with the Transport and Chemical Evolution-

Pacific (TRACE-P) (Jacob et al. 2003) in 2001, worked to quantify the spatial and vertical distribution of aerosol concentrations, properties, formation, and evolution over the western Pacific. Most recently, the Pacific Exploration of Asian Continental Emission (PEACE) campaign assessed the impact of changing emissions from Asia in 2002 (Parrish et al. 2004).

The transport of aerosols over the open Pacific has also been studied (Shaw 1980; Duce et al. 1980; Parrington et al. 1983; Uematsu et al. 1983). The Mauna Loa Observatory located to the Hawaiian Islands is an ideal location for studying the transport of dust aerosols across the Pacific Ocean from Asia. Shaw (1980) observed a 1-km thick dust layer at an altitude of 3.5 to 4.0 km with an aerosol optical depth (AOD) of 0.18 (Figure 3a) and a range of particle sizes from 0.5 to 5.0 μm over the Islands from late April to early May in 1979. Back trajectories revealed that the dust layer originated from the Gobi Desert about 9 days earlier (Figure 3b). Parrington et al. (1983) and Uematsu et al. (1983) found that dust loading in the mid-troposphere was heaviest over the Pacific during the spring months with a peak in April and May. Higher concentrations of dust were also found at higher latitudes and coincided with the prevailing westerly winds.

More recently, research has focused on the impact of dust transport on downwind continents, particularly on the United States' air quality and radiation budget (Gueymard et al. 2000; Husar et al. 2001; Tratt et al. 2001; Jaffe et al. 2003a, 2003b; VanCuren et al. 2002; Chin et al. 2007). In April 1998, a low-pressure storm moved through Mongolia into north-central China with surface winds over 20 m s^{-1} . Husar et al. (2001) tracked the dust that was picked up by the strong surface winds from its source in the Gobi Desert across China over the Pacific to the United States, and found that the dust was easily

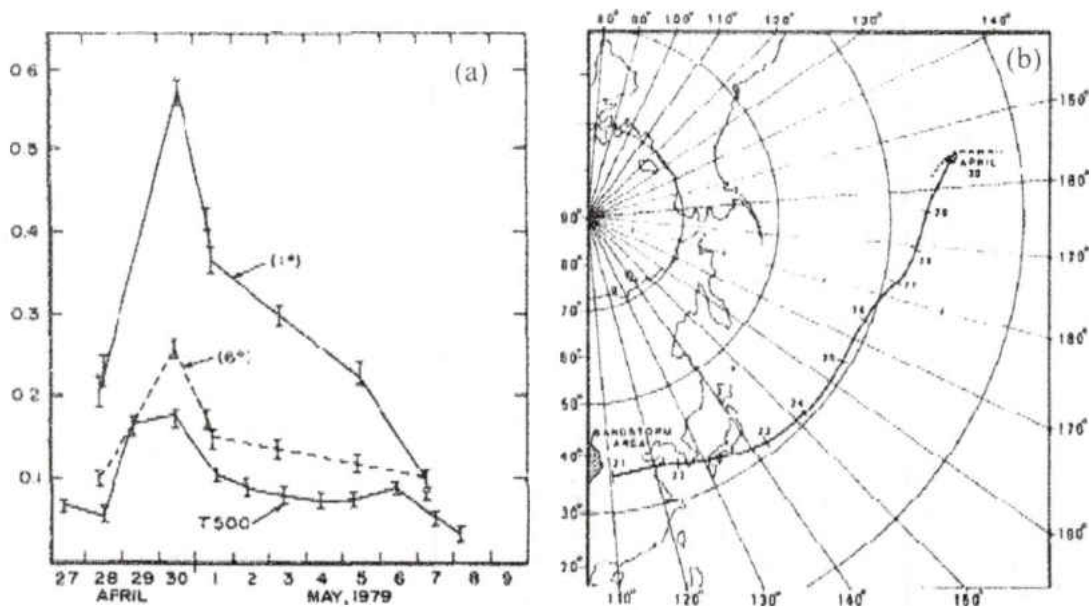


Figure 3. The temporal variation of (a) τ_{500} , the optical thickness above 3.6 km altitude and at 500 nm wavelength and (b) back isobaric trajectory at 500 hPa level. (Images from Shaw 1980).

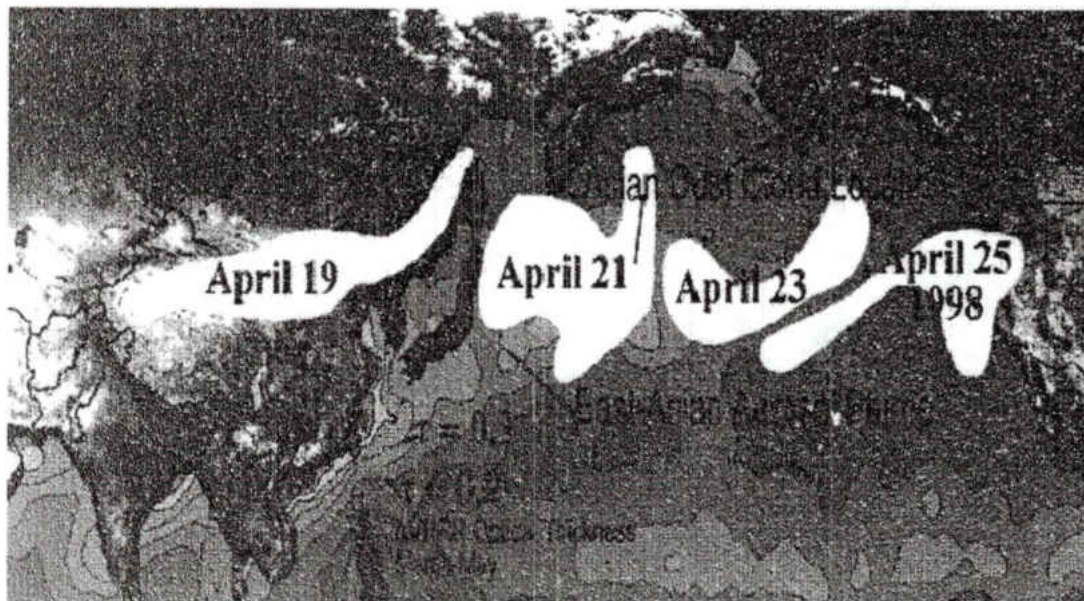


Figure 4. The Asian dust event of April 1998 as it traveled across the Pacific. The dust pattern was derived from satellite images. (Image from Husar et al. 2001).

traced during its journey due to its bright yellow color reflected in satellite images. The dust plume reached the West Coast of the U.S. within 6-7 days, meaning that the average transport speed of the aerosols was around 12 m/s (Figure 4).

The Facility for Atmospheric Remote Sensing in Salt Lake City, UT first measured the incoming dust by lidar, which indicated large non-spherical particles at 7.5 km about six days after the initial dust storm in East Asia. AOD values in the northwestern U.S. were between 0.4 and 0.5 (Husar et al. 2001), and further south, at San Nicolas Island, AOD ranged between 0.3 and 0.5 compared to AOD less than 0.1 just days before the event (Husar et al. 2001). This increase in dust aerosols over the region impacted the solar transmission. Gueymard et al. (2001) found that the amount of direct solar radiation reaching the ground decreased by 30% in Oregon during the same time period.

Subsidence from the mid-troposphere to the surface along the West Coast allowed the dust plume to partially dissipate over the area for two days. There is some evidence that the dust was transported as far east as the Atlantic coastline of the U.S. and was also visible in Minnesota. The strength of this event impacting the U.S. was uncommon as it caused two to three times higher dust concentrations than any other event during the previous ten years.

To further improve our understanding of sources and sinks of environmentally important gases and aerosols through the constraints obtained by atmospheric observations, NASA led a field experiment called the Intercontinental Chemical

Transport Experiment – Phase B (INTEX-B¹) during the spring of 2006 over the eastern Pacific Ocean (Singh et al. 2006). The major goals of INTEX-B were to quantify the transpacific transport and evolution of Asian dust to North America and assess its implications for regional climate. In this study, the physical and optical properties of Asian dust are reported, as well as its strength and evolution from its source near the Gobi desert to its sink in North America during INTEX-B. Aerosol properties and surface and top-of-atmosphere (TOA) radiation budgets are analyzed during clear-sky (clean, no dust) periods first, then these clear-sky values are used as a baseline to select the strong and weak dust events, and finally these values are summarized by their mean and standard deviation in Table 1 (See Chapter IV). A combination of different datasets from surface (Asia and North America), satellite (Terra/Aqua), and aircraft (University of North Dakota [UND]/NASA DC-8) observations, as well as from forward trajectories from the NOAA HYSPLIT model are used to track and analyze these events. From this integrated dataset, the goal of this study is to contribute to the understanding of Asian dust and its impact on regional and global climate.

¹ INTEX-B, the second phase of the main field experiment called INTEX-North America, was a two-part field experiment with the first half of INTEX-B conducted over Mexico, but for this paper, INTEX-B here only refers to the second half of the campaign over the eastern Pacific Ocean.

CHAPTER II

DATA AND METHODOLOGY

Several data sets have been collected and used to analyze Asian dust in this study. Surface observed/retrieved AOD, solar irradiance, and Angström exponent were collected from the East Asian Study of Tropospheric Aerosols: an International Regional Experiment (EAST-AIRE) and the Aerosol Robotic Network (AERONET) for China, and only from AERONET for North America. The satellite AOD and TOA albedo were derived from the Moderate Resolution Imaging Spectroradiometer (MODIS) and Clouds and the Earth's Radiant Energy System (CERES) observations, respectively, on the Terra and Aqua satellites. The UND/NASA DC-8 aircraft participated in the INTEX-B field mission, and for this study, the NASA Langley Airborne Differential Absorption Lidar (DIAL) and TSI 3563 integrating nephelometer data were used. The surface, satellite and aircraft data were collected during the period of April – May 2006 for this study, and are discussed in the following three subsections.

Surface

China

Radiation and aerosol information in China were collected at Xianghe (39.753 °N, 116.961 °E) as part of the EAST-AIRE project (Figure 5). The observatory is located between two megacities, with Beijing 70 km to the northwest and Tianjin 70 km to the southeast. Due to its proximity to these two megacities, this site experience

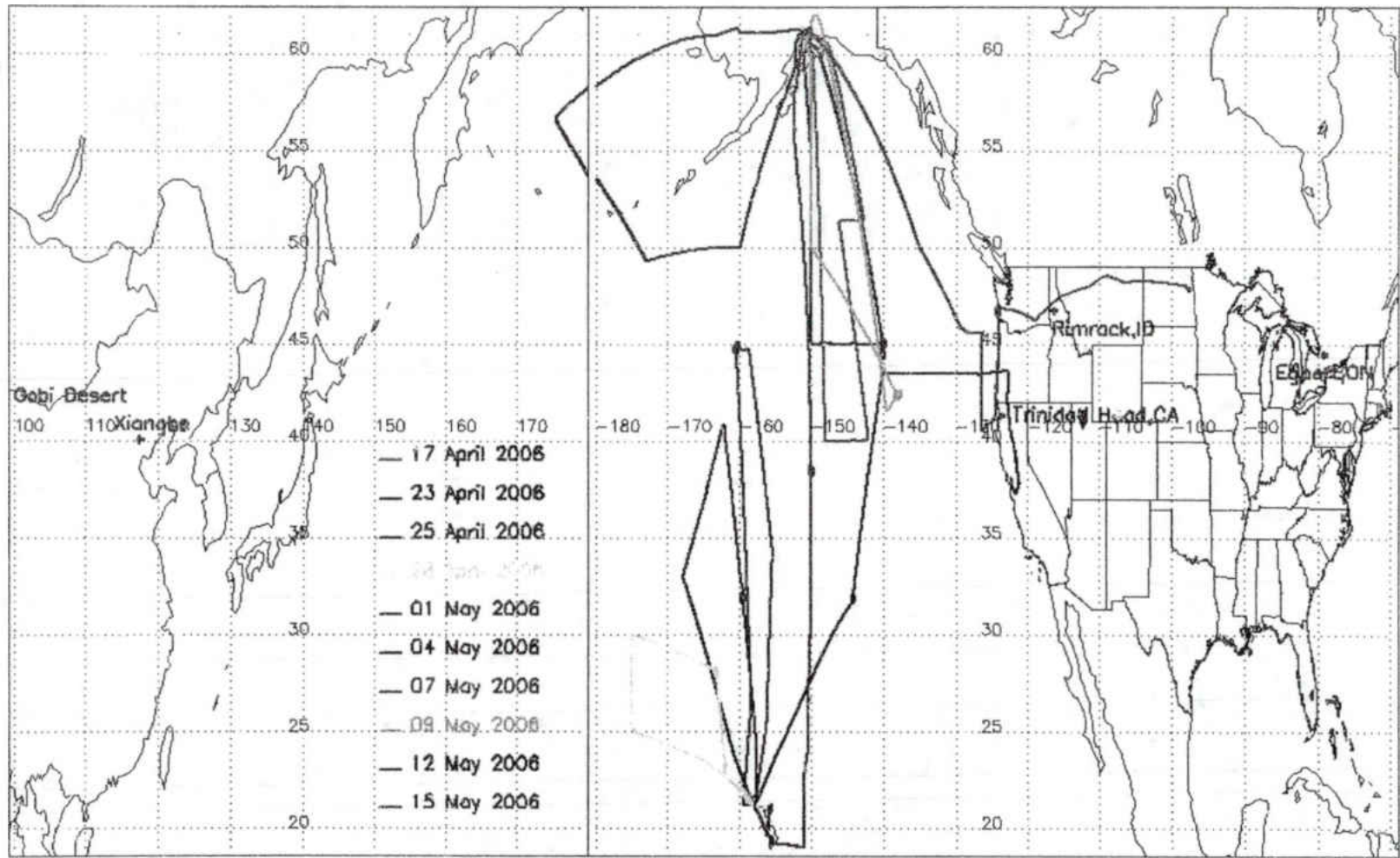


Figure 5. A map showing all surface sites (Xianghe, China; Trinidad Head, CA; Rimrock, ID; Egbert, ON) used during this study and all ten UND/NASA DC-8 flight tracks during INTEX-B. The Gobi Desert is also marked.

anthropogenic pollutants; however, it is also an ideal location for detecting dust aerosols originating from the Gobi desert. Dust particles have different characteristics that are easily identified from smaller anthropogenic aerosols and are discussed in Chapter III. This site has been taking continuous measurements of various surface radiation and aerosol quantities since it began operation on 21 September 2004. The total, direct, and diffuse downwelling shortwave (SW) radiation were measured at a 1-min temporal resolution with Kipp and Zonnen's CM21 and CM11 radiometers, a normal incidence pyrheliometer (NIP), and a black and white pyranometer, respectively, with an uncertainty of $\sim 5 \text{ Wm}^{-2}$. (For detailed information about EAST-AIRE, see the JGR 2007 special issue, e.g., Li et al. 2007).

As a part of the Aerosol Robotic Network (AERONET) (Holben et al. 1998), aerosol optical depth (AOD) was derived from Cimel-318 sun photometer measurements. The sun photometer is a multi-channel, automatic sun-and-sky scanning radiometer with a spectral range between 340 and 1020 nm and a total uncertainty under cloud-free conditions of $< \pm 0.01$ for $\lambda > 440 \text{ nm}$ and $< \pm 0.02$ for shorter wavelengths. The AOD values were retrieved at seven discrete wavelengths (340, 380, 440, 500, 670, 970, and 1020 nm) and were taken 30 seconds apart to create a triplet observation per wavelength used in the cloud-screening process. The triplet observations were made at 15-minute intervals in order to discriminate clouds in the variation of the triplet since the temporal variation of clouds is typically greater than that of aerosols. If any clouds were missed by the triplet observations, these outliers were removed by inspecting the AOD data for possible cloud contamination. Therefore, the AOD values used in this study exclude

most cloud-contaminated data. The Angström exponent (AE) (i.e. the slope of the spectral optical depth) was calculated by applying a linear regression to spectral sun photometer measurements as a function of wavelength on a logarithmic scale. For this study, only level 2.0 data (cloud-screened and quality-assured) were used.

Images from the total sky imager (TSI-440) were also used to help determine cloudy or dusty conditions at Xianghe. The TSI-440 takes snapshots of the sky on a continuous 1-minute basis each day from sunrise to sunset. Given the high frequency of images captured, a movie of sky conditions was generated for each day (Li et al. 2007). Since atmospheric aerosols tend to be less variable than clouds, it is a useful visual tool in separating aerosol-loaded clear-sky events from cloudy events, such as thin cirrus. Figure 6 is an image of the instruments at the Xianghe, China station.

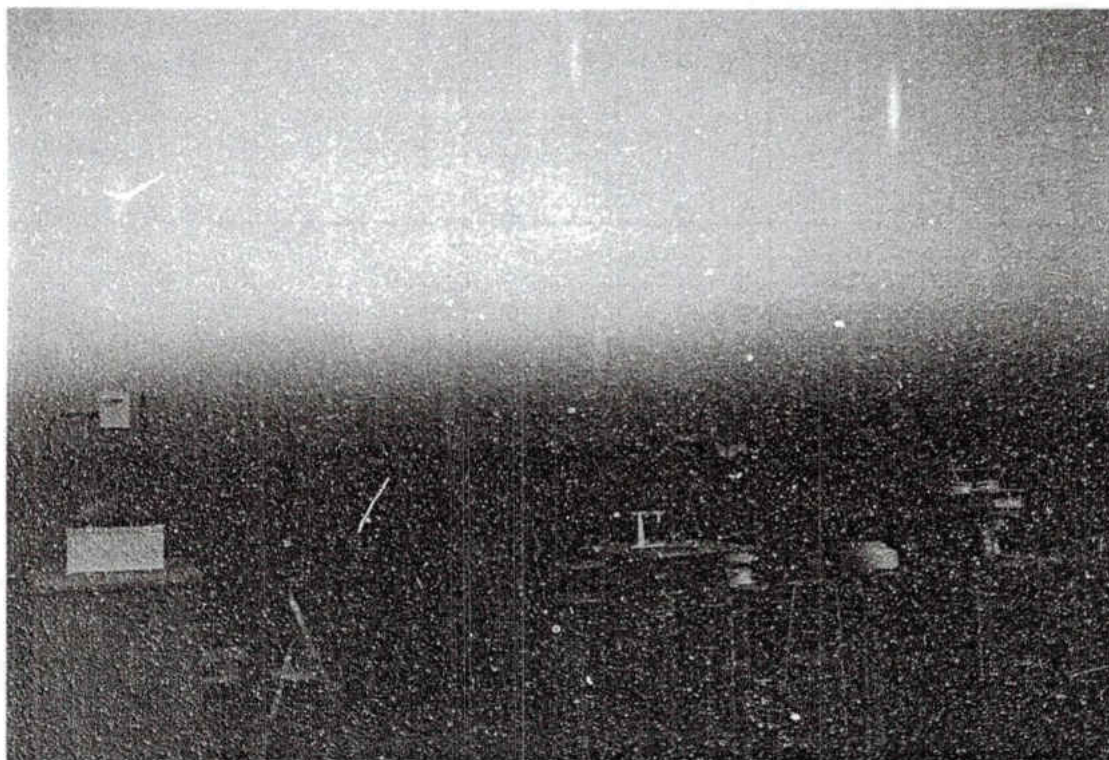


Figure 6. Instruments at the Xianghe, China surface station. (Image from EAST-AIRE 2008).

North America

To track the Asian dust events to their sink, as well as to study their strength and evolution, AOD and AE were collected at specific AERONET sites (Figure 5) in North America: Trinidad Head, CA (41.054°N, 124.151°W); Rimrock, ID (46.488°N, 116.992°W); and Egbert, ON, Canada (44.226°N, 79.750°W). These three sites were chosen because of either their remote location (little to no anthropogenic influence from nearby cities under prevailing synoptic conditions), their locations within the trajectory of the dust from Asia, and/or their instruments' high uptime during April – May 2006.

Satellite

The satellite datasets used in this study were the Terra Edition2B and Aqua Edition1B CERES Single Scanner Footprint (SSF) products. They include the “Rev1” calibration adjustment to the CERES SW record (Matthews et al. 2005), which was performed to account for optics contamination during the first few years in orbit. The CERES instruments on the Terra and Aqua satellites measure radiances that are converted to broadband fluxes using ADMs sampled and optimized for each satellite orbit. Estimated uncertainties in the solar-reflected, single field-of-view, instantaneous radiative fluxes at the TOA (SW_{toa}^{\uparrow}) are 13 Wm^{-2} (Chambers et al. 2002; Loeb et al. 2003). The SSF combines CERES broadband flux measurements at a 20-km resolution with coincident, sub-sampled 1-km MODIS cloud and aerosol retrievals (Wielicki et al. 1996; Ignatov et al. 2005). These datasets include the MODIS-retrieved visible (550 nm) AOD (MOD04 on Terra; MYD04 on Aqua) and CERES-derived TOA albedo over the ocean and land. The MODIS AOD product uses sophisticated cloud screening and aerosol retrieval algorithms developed by the MODIS cloud and aerosol groups with

uncertainties of 0.05 over land and 0.03 over ocean (Tanré et al. 1997; Ackerman et al. 1998; Martins et al. 2002; Remer et al. 2005). The satellite images used in this study are a composite of one day's worth of Terra or Aqua overpasses from 20° – 65°N and 90°E to 110°W that covers both source and sink regions.

UND/NASA DC-8 Aircraft

The UND/NASA DC-8 aircraft platform measured aerosol properties remotely and in-situ during ten flights (Figure 5) between 17 April and 15 May 2006 with a total of 85 hours over the central Pacific Ocean between Hawaii and Alaska. For this study, the DIAL and nephelometer measurements were used to determine the location of dust in the atmosphere. The integrated measurements from these two instruments provide a complete picture of dust location and strength, both remotely as well as in-situ.

DIAL

The DIAL system aboard the NASA DC-8 aircraft (Figure 7) made simultaneous ozone and aerosol backscatter profile measurements with four laser beams: two in the ultraviolet (UV) for ozone and one each in the visible and infrared for aerosols (Browell et al. 1998). These laser beams point both upwards and downwards from the aircraft and have a vertical resolution of 30 m, a horizontal resolution of 2.3 km and a 10-second temporal resolution along the DC-8 flight track. Only the visible (588 nm) and near-infrared (1064 nm) aerosol scattering ratios, total depolarization and aerosol wavelength dependence (1064/588 nm) were processed by the NASA Langley's Lidar Application Group.

The lidar scattering ratios in both visible and near-infrared wavelengths at altitude z can be calculated by:

$$R(z) = \frac{\beta_1(z) + \beta_2(z)}{\beta_2(z)}, \quad (1)$$

where $\beta_1(z)$ and $\beta_2(z)$ are the backscattering coefficients by aerosols and air molecules at altitude z , respectively. Under very low aerosol loading conditions, $R(z)$ is close to unity (Murayama et al. 2001). The depolarization ratio is defined as the ratio of the backscattered signals of the perpendicular to the parallel polarization of backscattered light, as measured with the emitted linear polarized laser. The depolarization ratios during the dust events are higher (>10%) than those under clear-sky background conditions.

Nephelometer

The TSI 3563 integrating nephelometer measured the scattering coefficients in-situ during INTEX-B. The nephelometer measures the amount of light scattered by the aerosol and then subtracts the light scattered by the walls of the measurement chamber, light scattered by the atmospheric gasses present (Rayleigh scattering), and the electronic noise inherent to the detector system.

The scattering coefficients have been corrected to 0-180° from the nephelometer detection angles (7-170°) based on the Anderson and Ogren (1998) method, and a 10-second average was applied to decrease instrument noise. The scattering coefficients were plotted as a function of time and height in order to create scattering coefficient profiles to easily compare with the DIAL images.

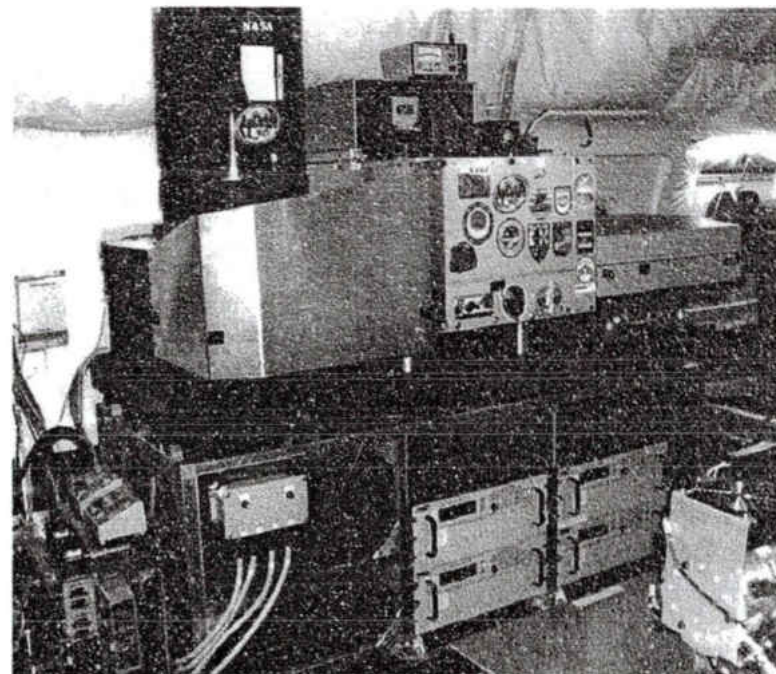
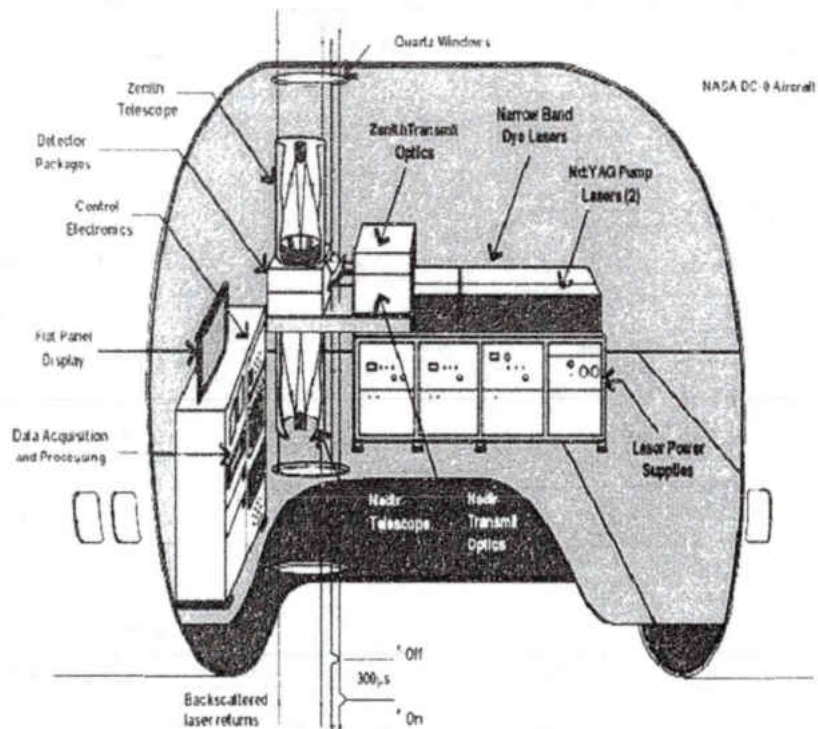


Figure 7. Schematic of the DIAL system is shown on the left and a picture of the DIAL system on the DC-8 aircraft is shown on the right. (Images from Browell et al. 2006).

CHAPTER III

RESULTS

In this study, the clear-sky (clean, no dust) events are selected based on surface and satellite observations and analysis of their physical properties and surface radiation budget. These clear-sky values are then used as a background to select the strong and weak dust events in their source region during the period of April-May 2006. Two days of clear-sky events, six days of strong dust cases, and five days of weak dust cases were selected, and their mean and standard deviation values are summarized Table 1 (See Chapter IV, Discussion). One event from each category is presented here. Forward trajectories are also used to track the strong and weak dust events to the eastern Pacific, where these events were observed by the DC-8 lidar and nephelometer and satellite measurements.

The criteria for selecting clear-sky events are: (a) downwelling direct SW surface fluxes are more than 80% of total global SW surface fluxes, (b) diffuse SW surface fluxes are less than 20% of total global SW surface fluxes, (c) AE is greater than one, and (d) AOD values retrieved from both surface and satellite are less than 0.4. Strong dust events are selected using the following criteria: (a) downwelling direct SW surface fluxes are less than 20% of total global SW surface fluxes, (b) diffuse SW surface fluxes are more than 80% of total global SW surface fluxes, (c) AE is less than 0.3, and (d) AOD values retrieved from both surface and satellite are greater than 1. Weak dust events fall between the clear-sky and the strong dust criteria. TSI-440 movies and

MODIS visible images confirm that all events (clear, strong, and weak) were not contaminated by clouds.

Clear-sky (Clean, No Dust)

To determine the baseline and provide the background values for studying Asian dust at Xianghe, China, a clear-sky event on 10 May 2006 is analyzed first using surface and satellite data. As shown in Figure 8a, the maximum total, direct, and diffuse downwelling SW fluxes are 1003 Wm^{-2} , 849 Wm^{-2} , and 160 Wm^{-2} , respectively. These values are representative of typical meteorological conditions of a cloud-free day, when aerosol loading is low and SW scattering/absorbing is mainly due to atmospheric molecules. The surface AOD and AE values are nearly constant throughout the whole day with averages of 0.17 (at $\lambda=500 \text{ nm}$) and 1.26, respectively, indicating that small particles are present (Figure 8b).

The averaged MODIS AOD and CERES TOA albedo for the $20^\circ \times 20^\circ$ grid box (Figure 9) are given in the upper right corner of the images. Although the averaged AOD (0.58 and 0.35) and TOA albedo (0.31 and 0.30) over the grid box are much higher than expected, the AOD and TOA albedo directly over the surface site are much lower (~ 0.1) than the averages of the grid box. This is consistent with the sun photometer average of 0.17. Background values for MODIS AOD and albedo over the Pacific Ocean are 0.1-0.2. Most of the MODIS retrieved AOD are associated with low TOA albedo (cloud-free); in other words, if AOD values are not retrieved, then these are associated with high TOA albedo (clouds). This comparison indicates that the MODIS cloud mask does a good job in the cloud-screening process and is consistent with the CERES result. The MODIS visible image (Figure 10a) shows that the sky is clear with little aerosol loading

over the surface site but with some aerosols about 200 km south of the surface site (also shown in Figure 9) and clouds in the southeast region.

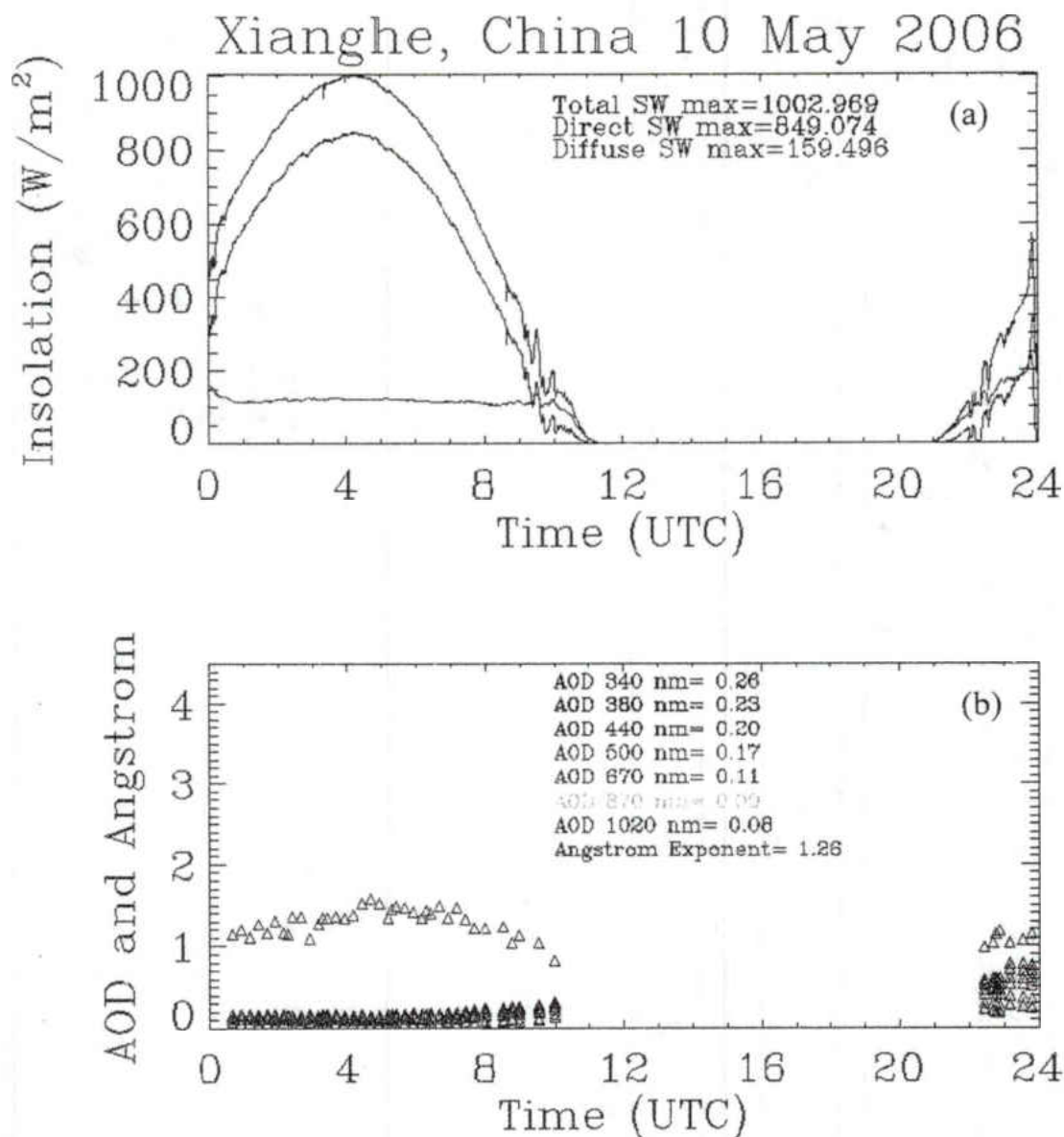


Figure 8. A time series of (a) insolation, (b) AOD, and Angström exponent over Xianghe, China for the clear-sky event on 10 May 2006. The maximum values for total (purple), direct (black), and diffuse (red) downwelling SW radiation and the mean values for Angström exponent and AODs from seven wavelengths.

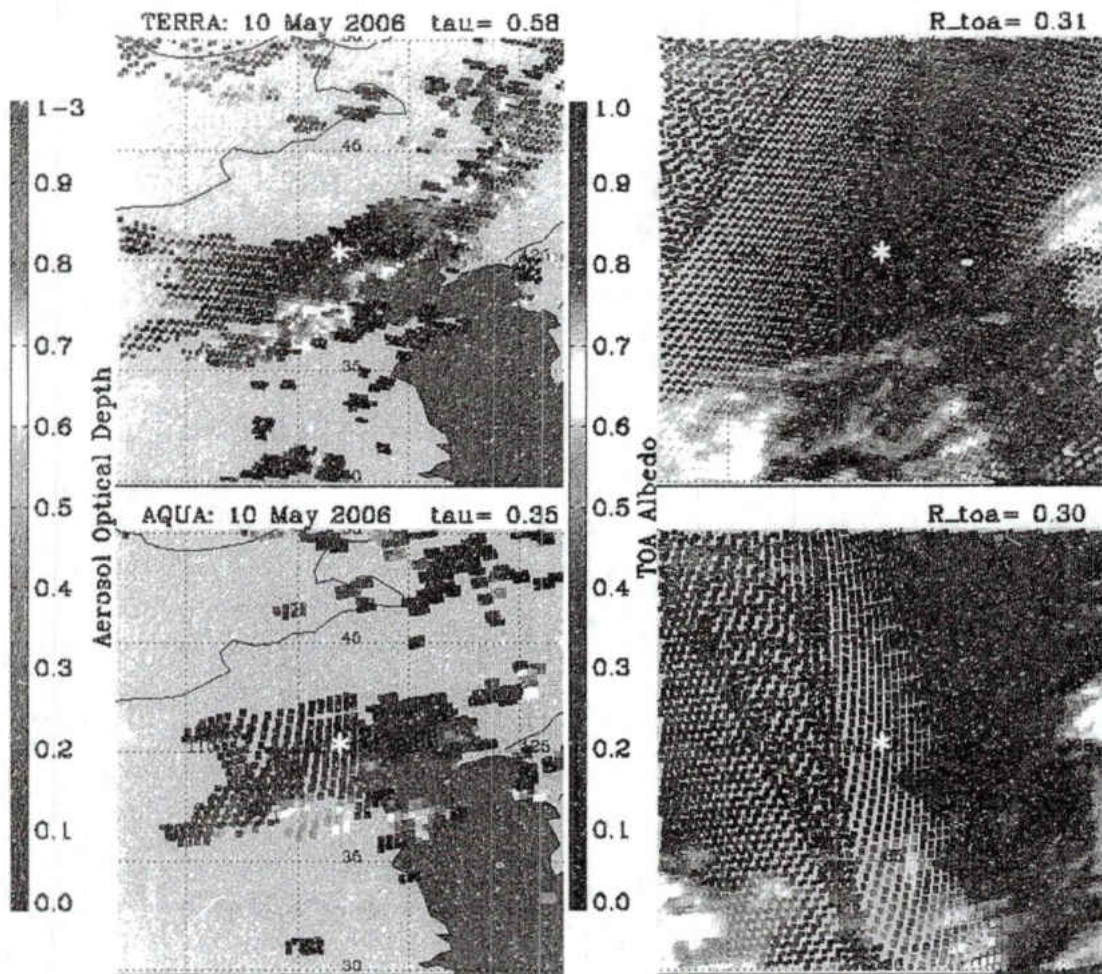


Figure 9. AOD (left two images) and TOA albedo (right two images) from Terra (top) and Aqua (bottom) satellites centered over Xianghe, China (white star) during the clear-sky event on 10 May 2006. Mean values are provided on upper right corner.

In Figure 10b, the NCEP one-day averaged sea level pressure analysis for this day shows a low-pressure system to the east and off the coast of China with high pressure building in from the northwest over the Gobi desert and Xianghe. The subsidence associated with the high pressure system, as well as a weak pressure gradient, kept wind speeds low at the surface and suppressed any dust particles from lifting high into the atmosphere.

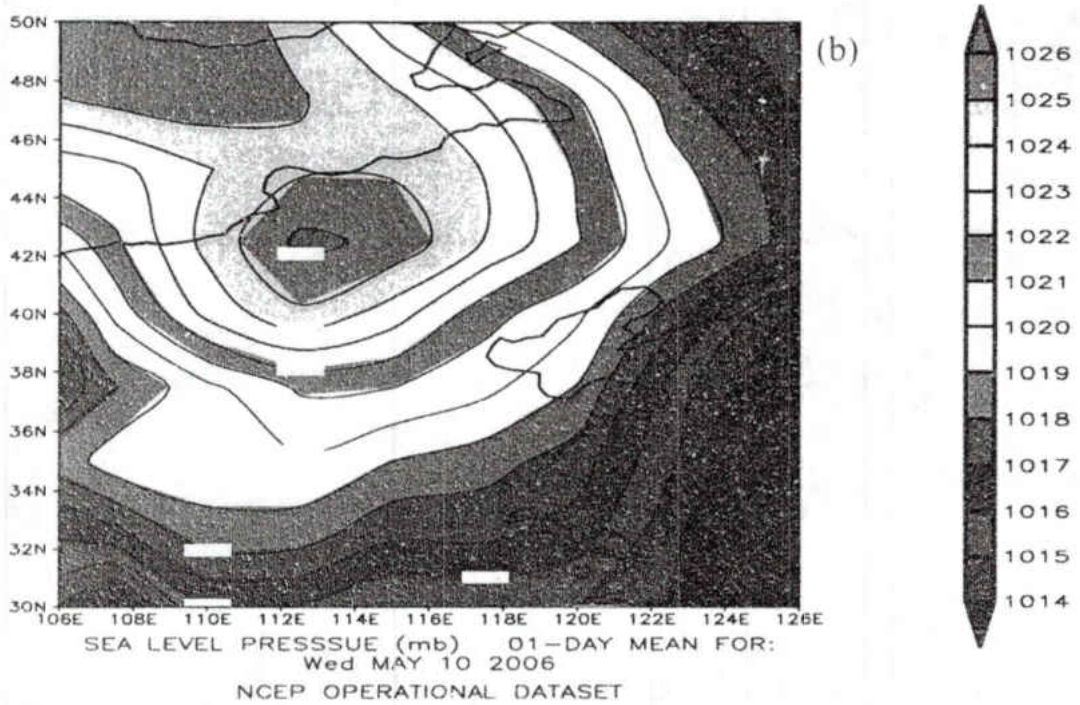
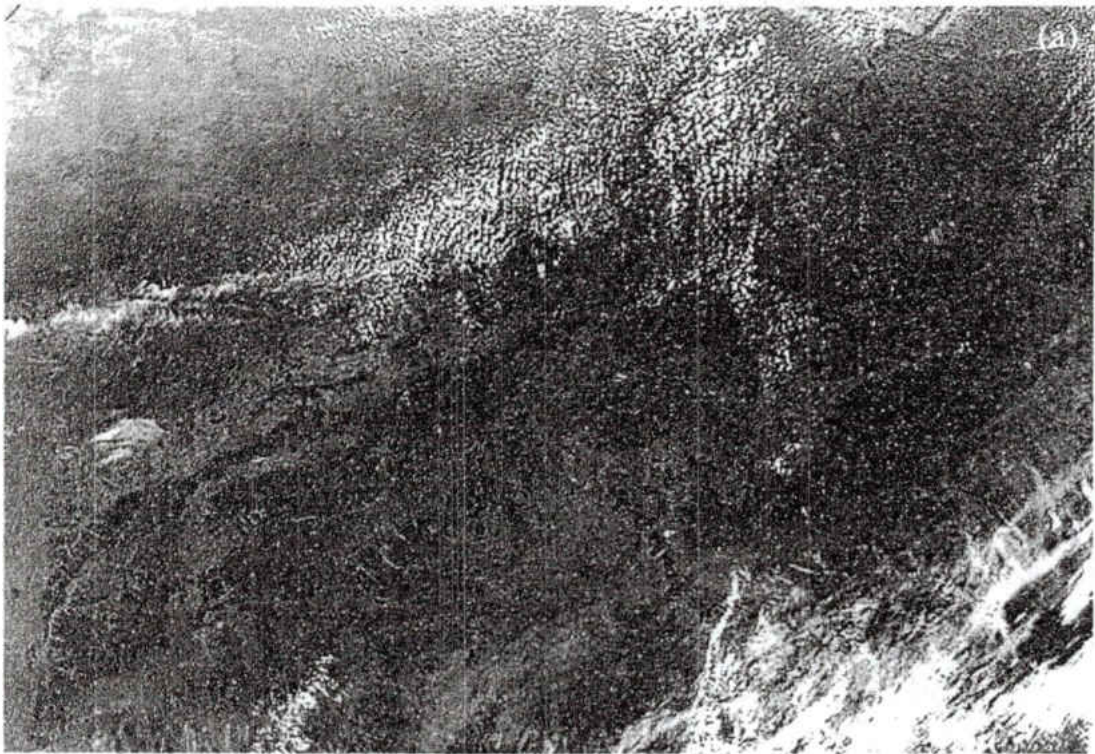


Figure 10. (a) MODIS visible image and (b) mean sea level pressure centered on Xianghe, China during the clear-sky event May 2006.

Dust Events

As discussed in the beginning of this section, both surface and satellite observations/retrievals were used to identify and classify dust events into two main categories: (a) strong and (b) weak in their source region. These dust events are tracked from their source region across the Pacific Ocean to North America using the Hybrid Single-Particle Lagrangian Integrated Trajectory (HYSPPLIT) forward trajectory model at three different altitudes: 3 km, 5 km, and 7 km AGL (Draxler et al. 2003). These three altitude levels were chosen because, according to Qiu and Sun (1994), aerosol dust particles can be transported east from China to the Pacific Ocean in the 3 to 7 km height range.

The UND DC-8 encountered the strong and weak dust events over the eastern Pacific Ocean on April 23-24 and April 17-18, respectively, and sampled them using the DIAL and nephelometer instruments. For all dust events, the DIAL aerosol scattering ratio at 1064 nm (AS-NIR), the aerosol scattering ratio at 588 nm (AS-VIS), and the total depolarization (Depol.) values all increase, whereas the aerosol wavelength dependence (1064 nm/588 nm; WD) decreases when compared to its relative clear-air surroundings. Since WD is inversely related to the particle size when compared to clear-air observations, WD will decrease. A higher scattering coefficient also indicates the presence of larger particles. As the dust settles out and spreads over a larger area, both Terra and Aqua AOD values over the eastern Pacific Ocean are lower than those over their source region but are still higher than the clear-sky values. Even though AOD is much lower over the eastern Pacific and North America, these dust events can still be

traced with the aid of forward trajectories and a comparison to the site's surface background values.

Strong Dust Event

An intense Asian dust storm passed over the Xianghe site on 17 April 2006 as shown in the MODIS visible image (Figure 11a). This dust event was driven by a strong low-pressure system (Figure 11b) that swept over Mongolia, the Gobi Desert, and then over Xianghe. Consistent with satellite observations, the TSI-440 movie at the Xianghe site showed no clouds passing over the site, indicating that dust almost completely obscured the Sun (i.e., no direct SW transmission). The strong low-pressure system and resulting cold front are consistent with other studies (Husar et al. 2001; Murayama et al. 2001; Shaw 1980; Duce et al. 1980) that show that this synoptic system configuration causes dust particles to be lofted into the mid-troposphere. The strong winds associated with the low-pressure system were great enough to lift the dust into and above the boundary layer (Gillette 1978), making long-range transport in the free atmosphere possible.

Figure 12a presents the total, direct and diffuse downwelling SW fluxes, and their corresponding maximum values at the Xianghe site on 17 April 2006. The downwelling direct SW surface fluxes are no more than 25 W/m^2 and diffuse SW radiation accounts for 90% or more of the total incoming solar radiation. The AOD and AE values over the Xianghe site are greater than 4.0 and less than 0.1 (Figure 12b) and are consistent with the surface SW observations. All observations indicate that the 17 April 2006 event is a strong Asian dust storm. The nearly diminished direct SW transmission can also be explained by radiative transfer theory ($T \sim e^{-\tau}$). Compared to the clear-sky maximum SW

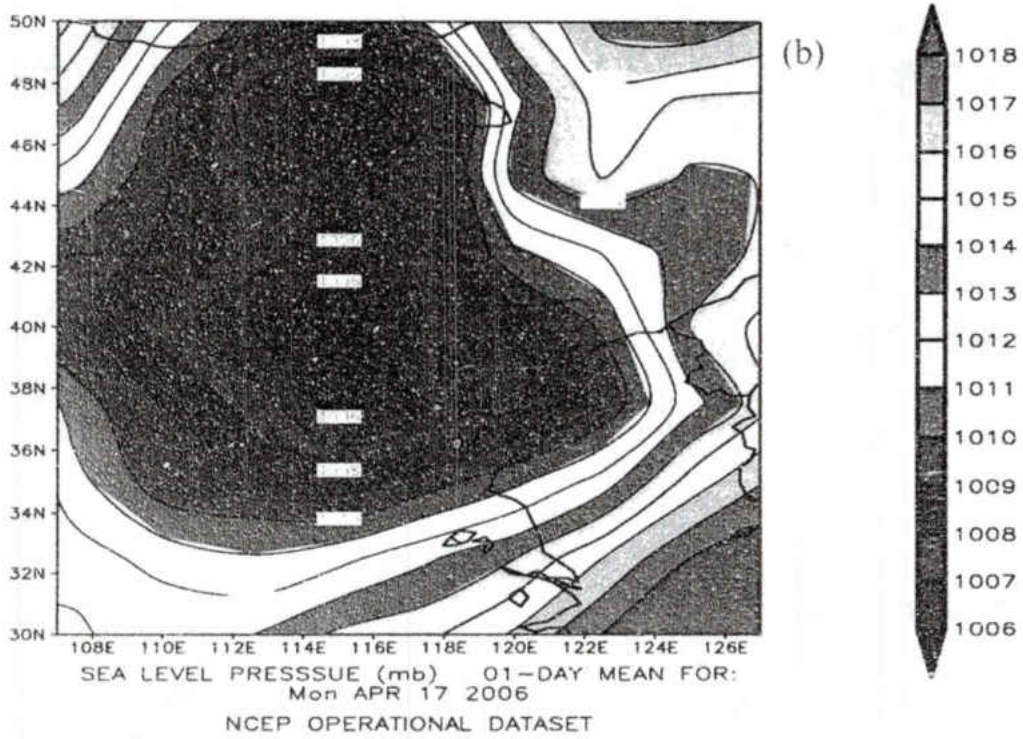
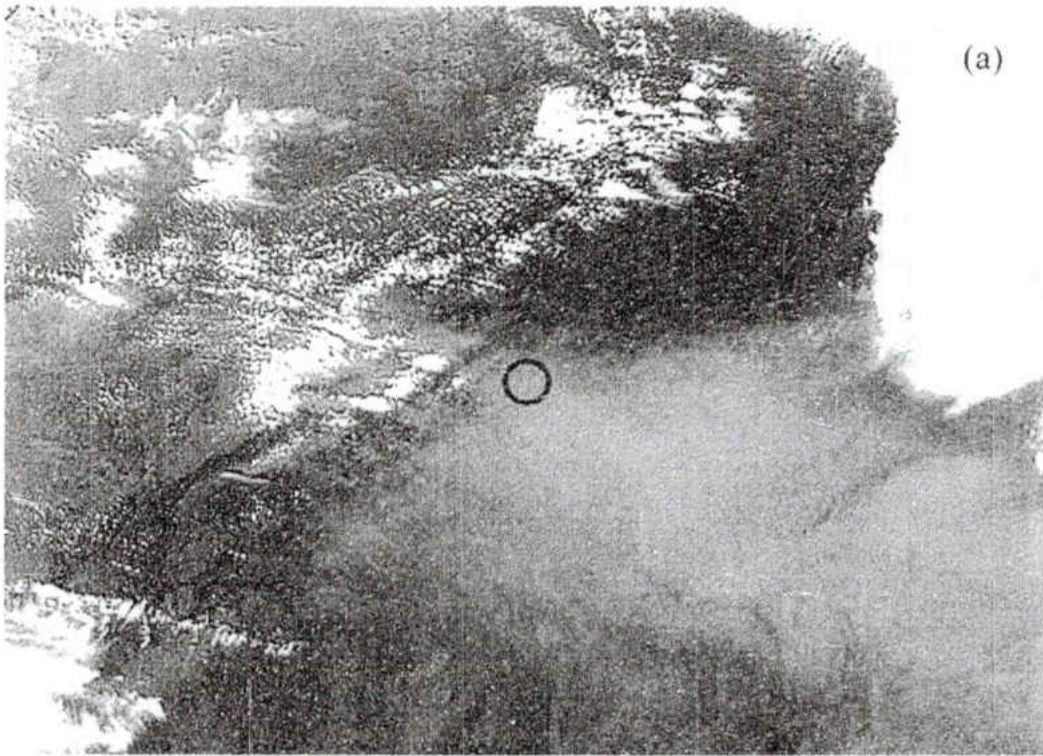


Figure 11. Same as in Figure 10 but for a strong dust event on 17 April 2006.

observations, total and direct SW transmissions were reduced 53% and 97%, respectively, whereas diffuse SW transmission increased 177%. The mean value for AOD increased from 0.17 (clear-sky average) to 4.0, and the AE dropped from 1.26 (clear-sky) to below 0.1. Xia et al. (2007) studied the effects of aerosols on the surface radiation budget in northeastern China and found that direct SW fluxes could be reduced up to -522 W/m^2 per unit of AOD with 66% of the reduction being offset by an increase in diffuse SW flux.

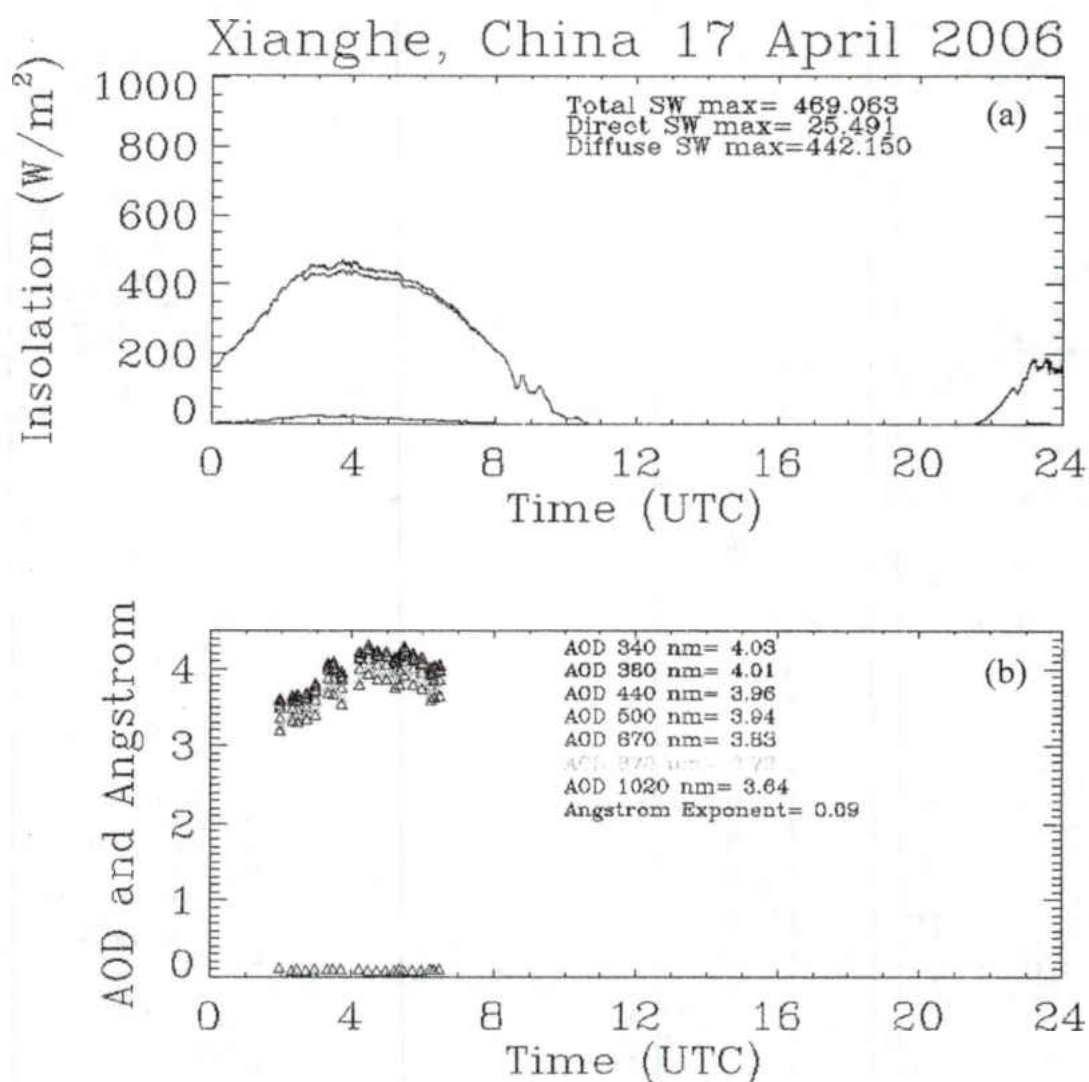


Figure 12. Same as in Figure 8 but for a strong dust event on 17 April 2006.

Although the averaged AOD values (Figure 13) over the grid box from both Terra and Aqua are not as large as the surface retrievals, the high AOD values just south of the Xianghe site correspond well with this dust event. The averaged TOA albedo is 25% over the surface site, which is an increase of 10% (absolute) from the clear-sky value. From radiative transfer calculations and observations in this study, increasing the AOD (up to 4) can slightly increase the TOA albedo but can significantly impact downwelling SW transmission, especially for direct SW radiation.

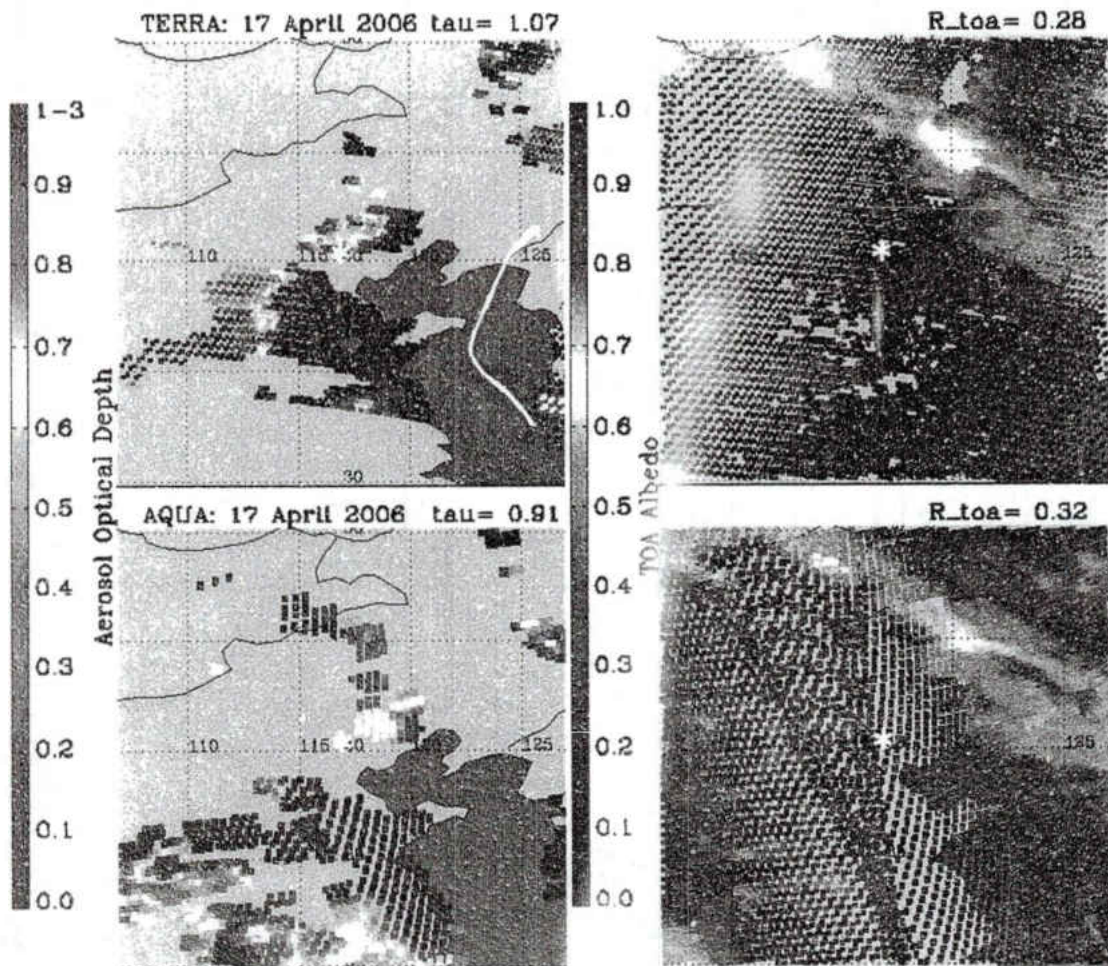


Figure 13. Same as in Figure 9 but for a strong dust event on 17 April 2006.

As the low-pressure system (Figure 11b) moved eastward over the Pacific Ocean, the dust was carried by mid-level winds (27 m s^{-1}) and experienced deformation. A 500 hPa ridge was positioned just west of the dateline (NCEP upper air analysis not shown here), and the dust followed this pattern eastward. MODIS and CERES retrievals confirm this pattern as AOD values can be tracked from their source in China to the eastern Pacific Ocean (Figures 14-19). On 18 April 2006 (Figure 14), the large AOD values (>1.0) over a large area indicate the expanse of the dust plume as it moves over Japan and the Pacific Ocean. The next day, following the upper level winds, the dust is located at 40°N and 160°E (Figure 15) where the AOD of the dust plume is still high ($0.8 - 1.0$) but starting to diminish as the larger particles settle out and dispersion of the plume over a larger area. By 20 April, the plume has elongated from the international dateline at 40°N to the northeast at 50°N and 140°W . Over the next two days (Figures 17-19), the southern part of the plume continues south as it becomes predominately influenced by the high pressure system north of Hawaii, and the northern branch continues eastward towards the west coast of the United States, trailing behind the low-pressure and cold front. The location of the dust on 22 April (Figure 18) is lost because there is no AOD data over that area but can be identified again on 23 April (Figure 19).

The MODIS AOD values in Figures 19 and 20 indicate that this dust event was located along the flight path (center of Figure 20 image). The center of Figure 20 is cloud-free where AOD values range from 0.36 to 0.47, possibly indicating the location of dust, while the north and southwest regions are cloudy, identified by GOES-W satellite images. Since the MODIS AOD values are much lower over the eastern Pacific Ocean than the observations over China because of the spreading of the dust cloud over a larger

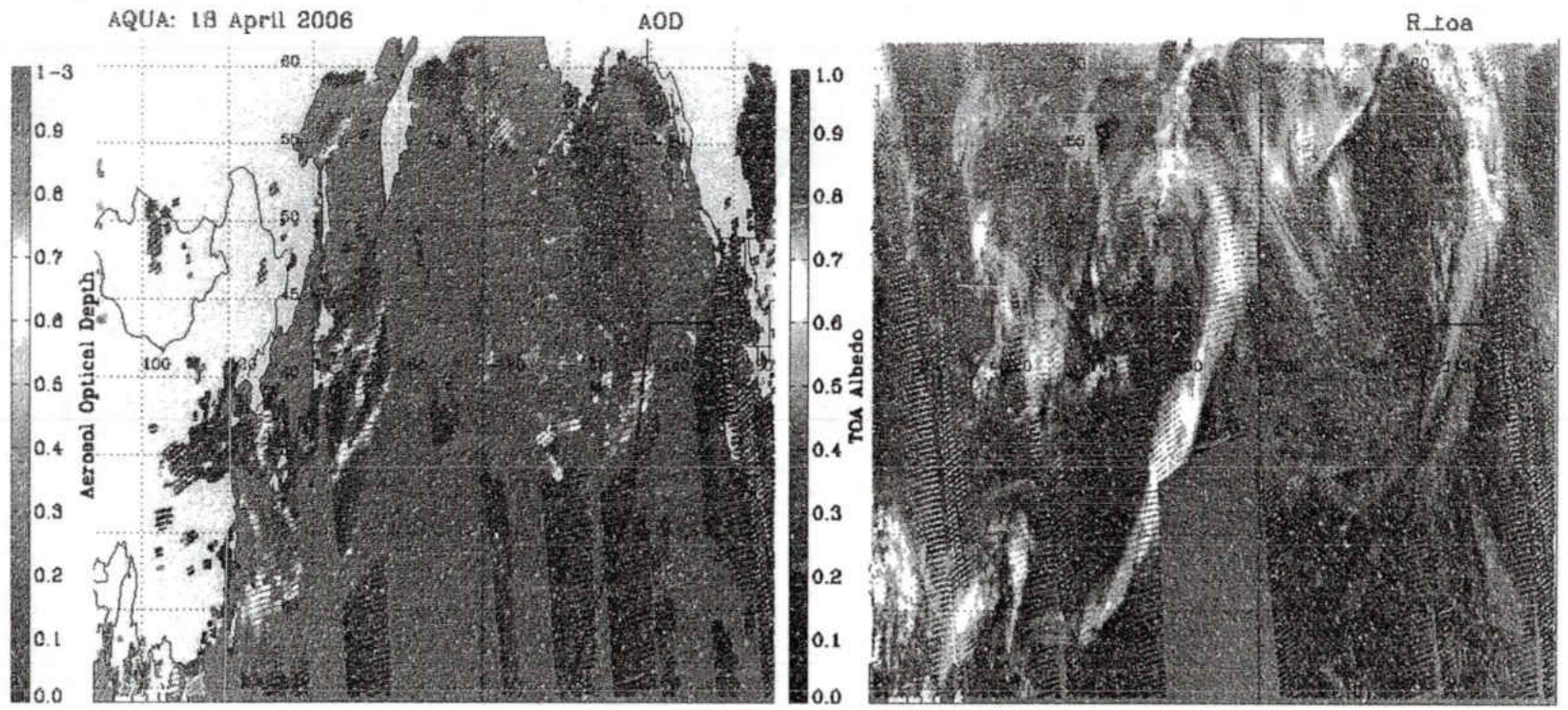


Figure 14. AOD (left) and TOA albedo (right) from Aqua over the Pacific Ocean for 18 April 2006. White star denotes Xianghe, China. Follow the dust transport from Figures 14-20.

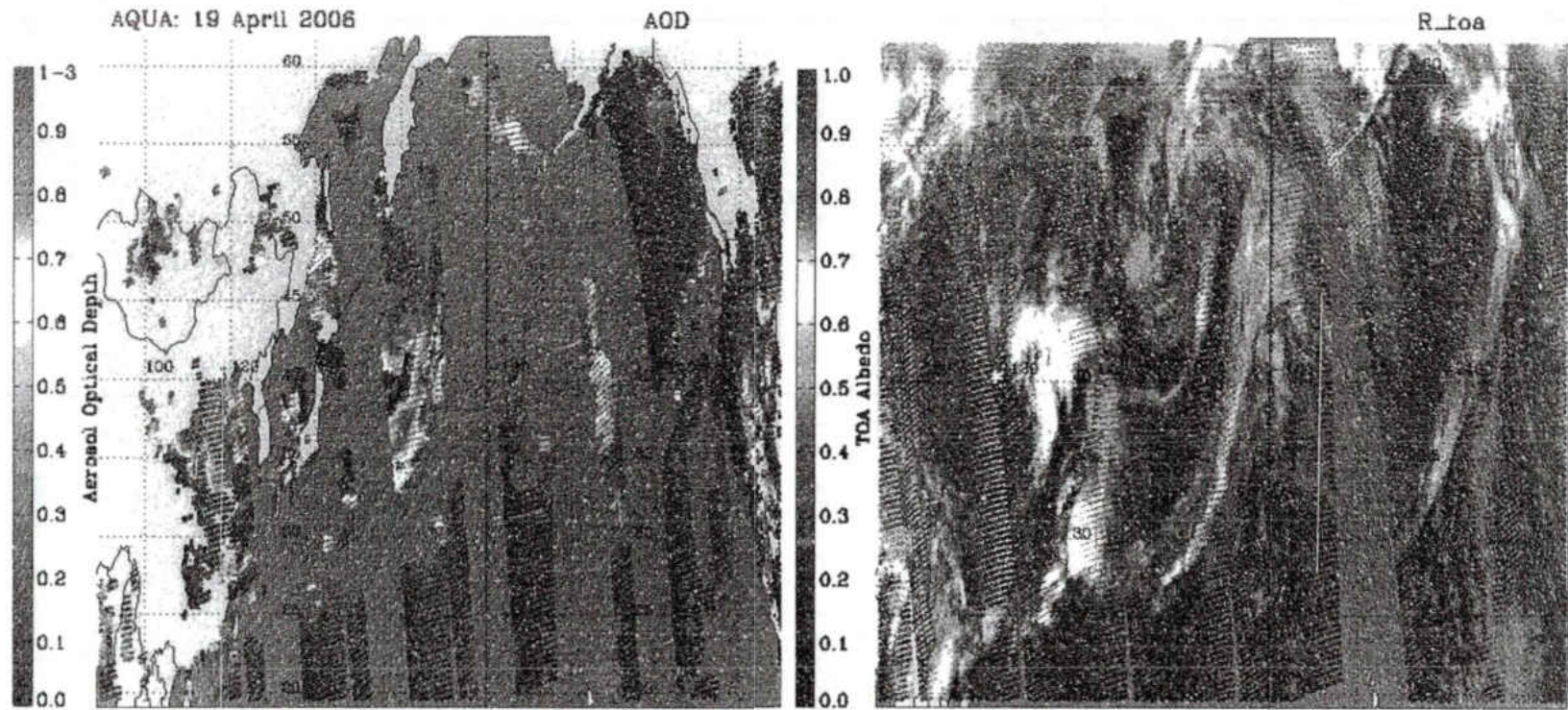


Figure 15. Same as in Figure 14 but for 19 April 2006.

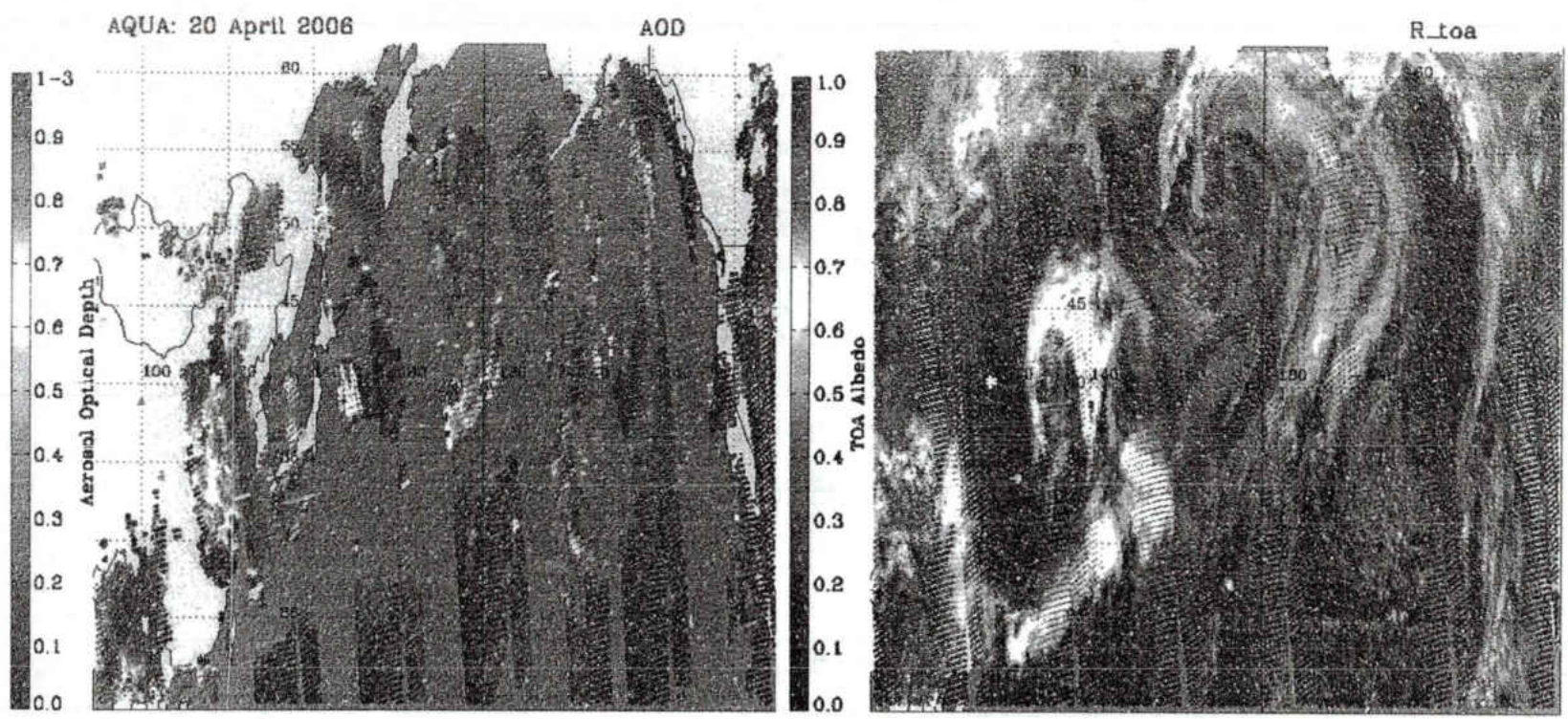


Figure 16. Same as in Figure 14 but for 20 April 2006.

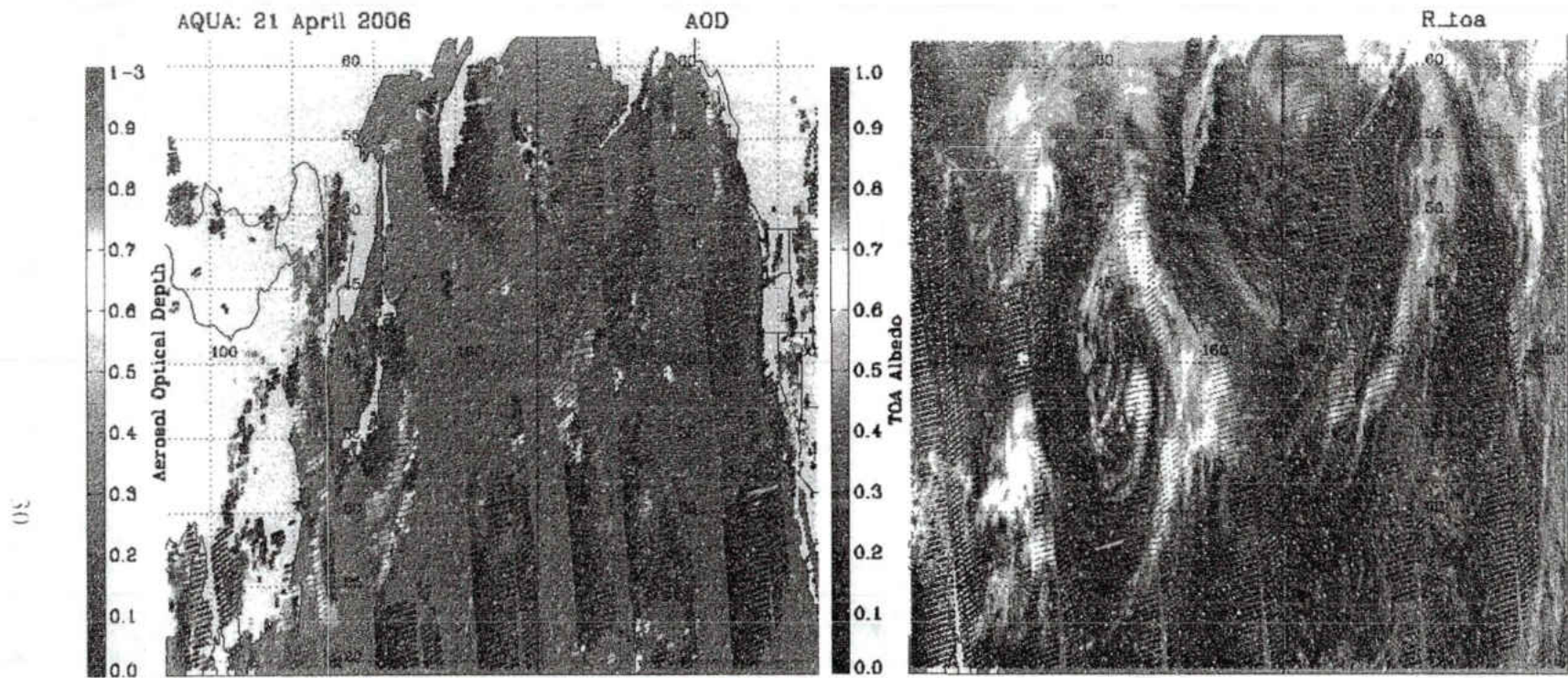


Figure 17. Same as in Figure 14 but for 21 April 2006.

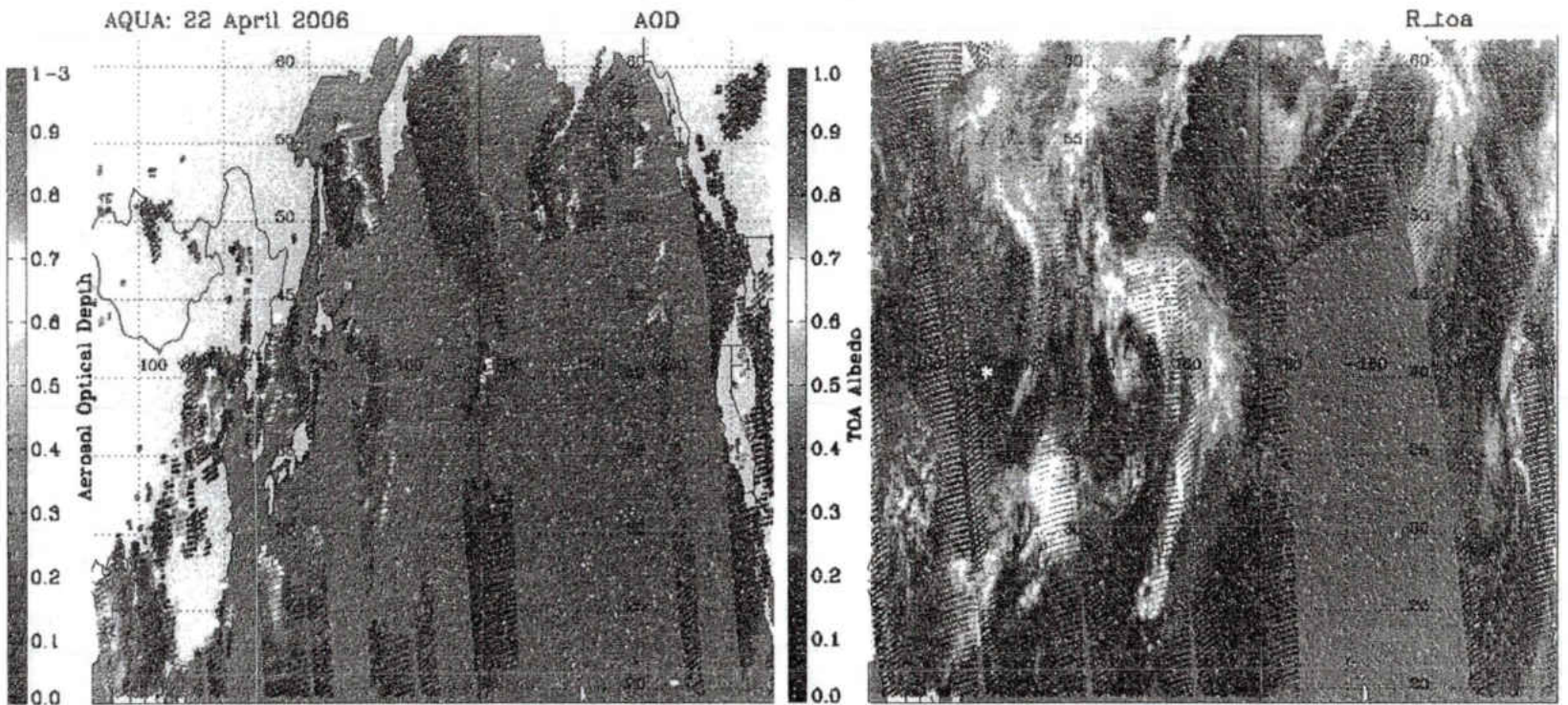


Figure 18. Same as in Figure 14 but for 22 April 2006.

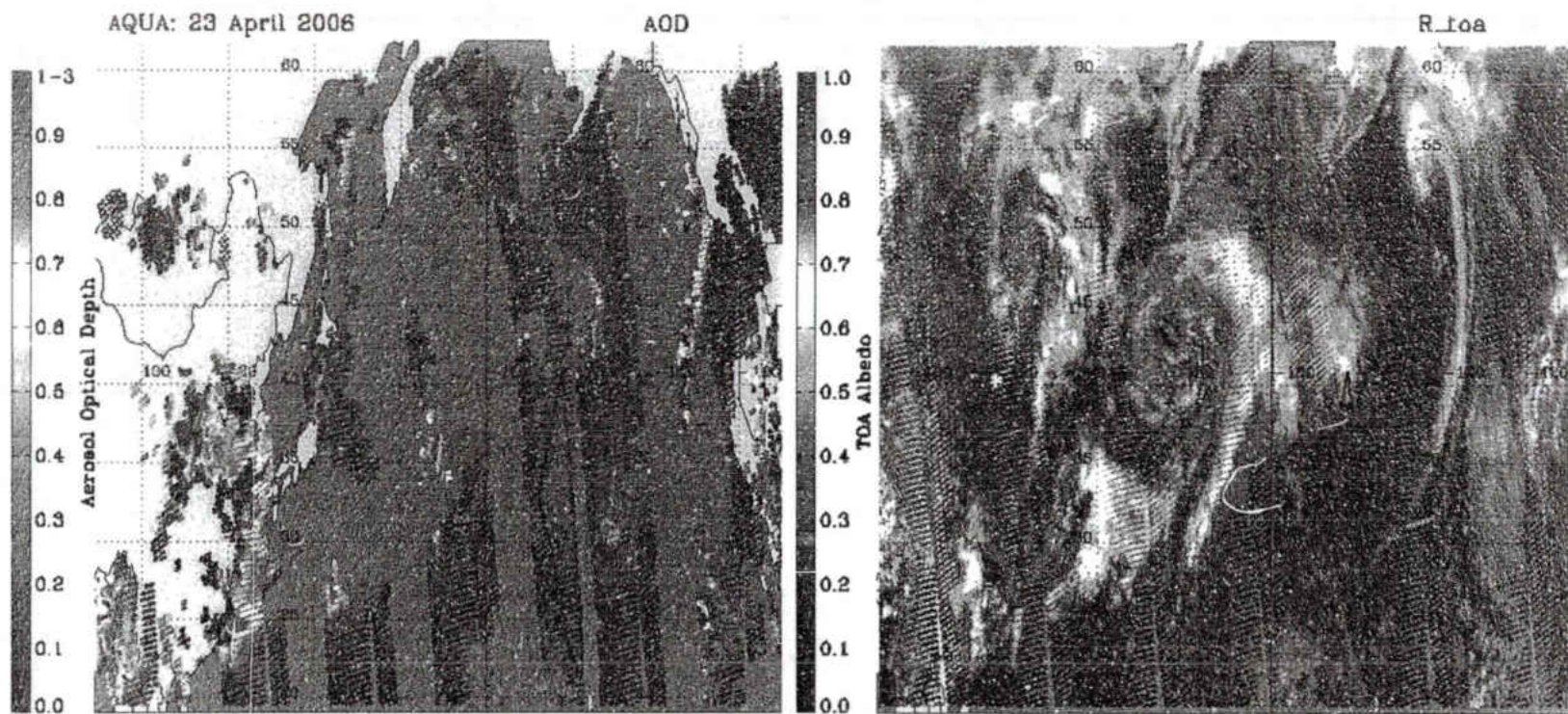


Figure 19. Same as in Figure 14 but for 23 April 2006. The flight track is overlaid in black. (See Figure 20 for a close up of the flight track).

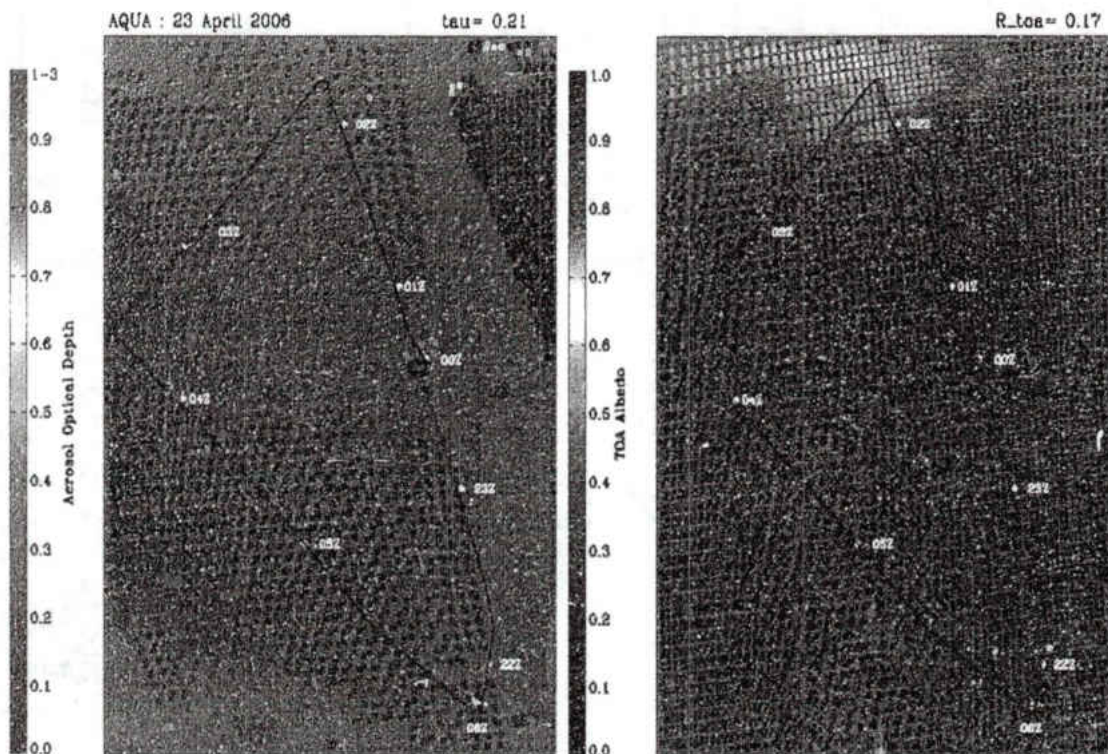


Figure 20. A close-up of the flight track coverage by the DC-8 on 23 April 2006 with MODIS AOD and CERES TOA albedo. Note the higher AOD values at 00 Z and 04 Z (time of DC-8 shown in white).

area, it is difficult to identify the dust event from satellite observations only. Therefore, it is necessary to use aircraft measurements to verify/validate the satellite retrievals.

The measurements made by the UND/NASA DC-8 aircraft captured this dust event over the eastern Pacific Ocean on 23-24 April 2006 (Figures 21 and 22) as it flew north-northwest from Hawaii (Figure 20). The DC-8 DIAL (Figure 21) image shows the time series of AS-NIR, AS-VIS, Depol., and WD observations from 22 UTC on 23 April to 6 UTC on 24 April 2006. Typical scattering AS-NIR and AS-VIS ratios for dust are 2-10 and 0.5-1, respectively, and depolarization is 20-30%. This dust layer was located just above the boundary layer stratus clouds at 1.5-4.0 km, and its averaged AS-NIR and AS-VIS ratios are 10.5 and 2.0, respectively. The averaged depolarization is 25%, and the

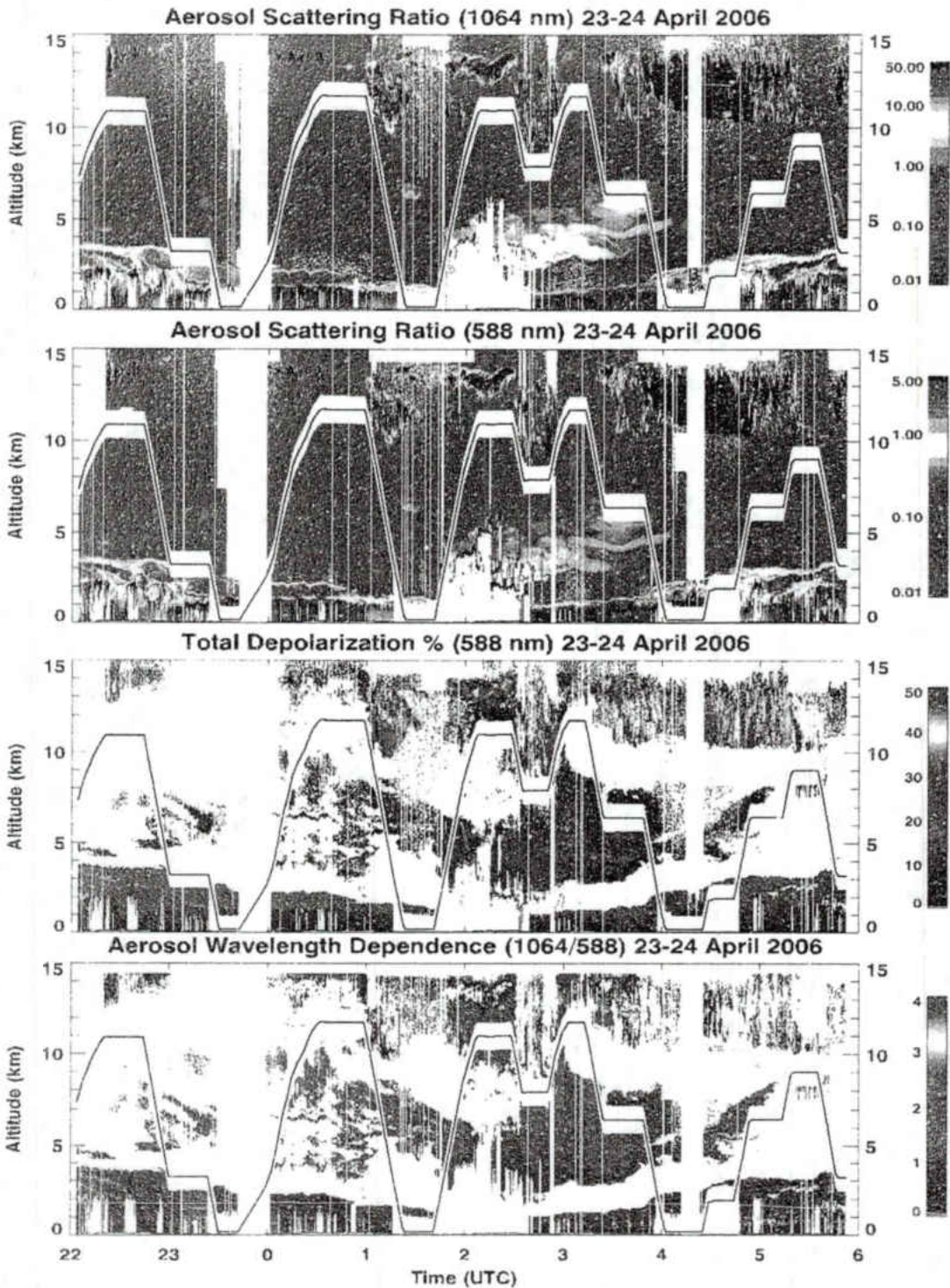


Figure 21. DC-8 DIAL for 23-24 April 2006 flight. From top to bottom are the AS-NIR, AS-VIS, Depol., and WVD. The flight altitude is the black line.

averaged WD is 0.6. The lower WD (less than 1.0) indicates that these particles are larger. The much higher AS-NIR and AS-VIS ratios >50.0 and >5.0 , respectively, above 10 km have been identified as cirrus clouds, not a dust layer, which has been confirmed by GOES-W images (not shown here) and through the application of the method described by Roskovensky and Liou (2005). From the DIAL image, the aircraft transects the dust plume at several points where in-situ measurements, like the nephelometer, were able to identify the dust particles.

The DC-8 nephelometer also observed this dust event in-situ and confirmed that the highest scattering coefficients were located at 1.5-3 km (Figures 22a-e). Higher scattering coefficients are indicative of larger aerosol particles. The first profile during the aircraft descent at 23:30 UTC in Figure 22a (or as seen in the DIAL image in Figure 21) shows the dust layer located at 2 km with the greatest scattering coefficient at 80 mm^{-1} , which is associated with the higher MODIS AOD values (~ 0.4 in Figure 20). Halfway through the flight (Figures 22b-d), the dust layer was low at ~ 1.5 km and thin with scattering coefficients as low as 38 mm^{-1} , and towards the end of the flight, the dust layer returned to heights above 2 km and with scattering coefficients of $80\text{-}100 \text{ mm}^{-1}$. The dust layer was at a higher altitude closer to Hawaii and as the aircraft traveled northward, the dust was lower in the atmosphere.

To further confirm the origin of this dust event from East Asia, a forward trajectory model (Figure 23), starting over the Xianghe site with three different heights (3, 5, and 7 km AGL), was run using the online HYSPLIT with reanalysis data (Draxler et al. 2003). It was assumed that any dust particles that were available for long-range transport were in the free-troposphere over Xianghe (Sun et al. 2001). The first trajectory

Nephelometer Total Scattering (550 nm) Profiles 23 April, 2006

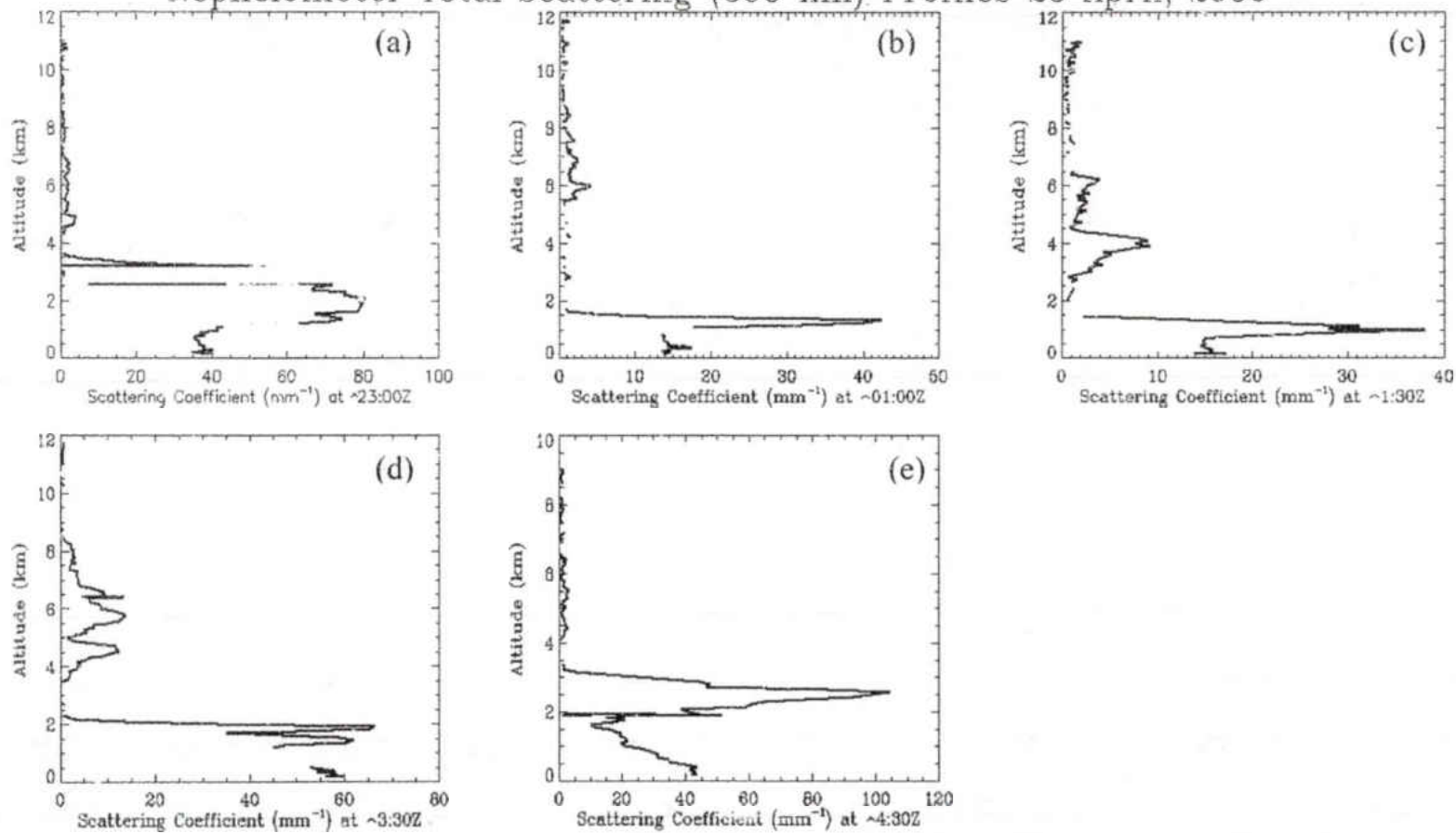


Figure 22. DC-8 nephelometer total scattering coefficient profiles at 550 nm for the 23-24 April 2006 flight. The approximate times of the profiles are as follows: (a) 23:00 Z, (b) 1:00 Z, (c) 1:30 Z, (d) 3:30 Z, and (e) 4:30.

(3-km) entrained into the low-pressure system and eventually settled out over the open Pacific. The trajectory that initialized over Xianghe at 7000 m followed the upper air pattern (ridge) for the first three days, and on the fourth day, this air mass started to subside and traveled south towards Hawaii where it entrained the dust into the surface high, as observed by the DC-8 over the eastern Pacific Ocean. This corresponds well to the location and time (Figures 14-19) of the dust plume as observed by MODIS and CERES.

The remainder of the dust that was not captured by the high-pressure system continued to move eastward in the upper atmosphere (the 5-km trajectory) towards the west coast of the United States/Canada (Figure 23). This dust-laden air mass descended over the northwest of North America on 23 April 2006 and was observed by the AERONET station at Rimrock, ID (Figure 24). In general, the dust originating from East Asia reached North America within seven days, which is consistent with previous studies (Shaw 1980; Uematsu et al. 1983; Husar et al. 2001). In Figure 24a, AERONET AODs showed a slight increase from before and after 23 April 2006 at Rimrock from an average of 0.05 to 0.1 at 500 nm. Although this is not as high (0.3-0.5) as Tratt et al. (2001) found during the April 1998 event at San Nicolas Island, the particular dust event described here was exceptional and heavily impacted the western United States for several days. The AE at Rimrock was below 0.5 with a mean of 0.32 (Figure 24b), which is indicative of larger characteristic particle sizes ($>1.0 \mu\text{m}$) (Angström 1929; Eck et al. 1999) and is consistent with the results found by Tratt et al. (2001).

NOAA HYSPLIT MODEL
 Forward trajectories starting at 00 UTC 17 Apr 06
 CDC1 Meteorological Data

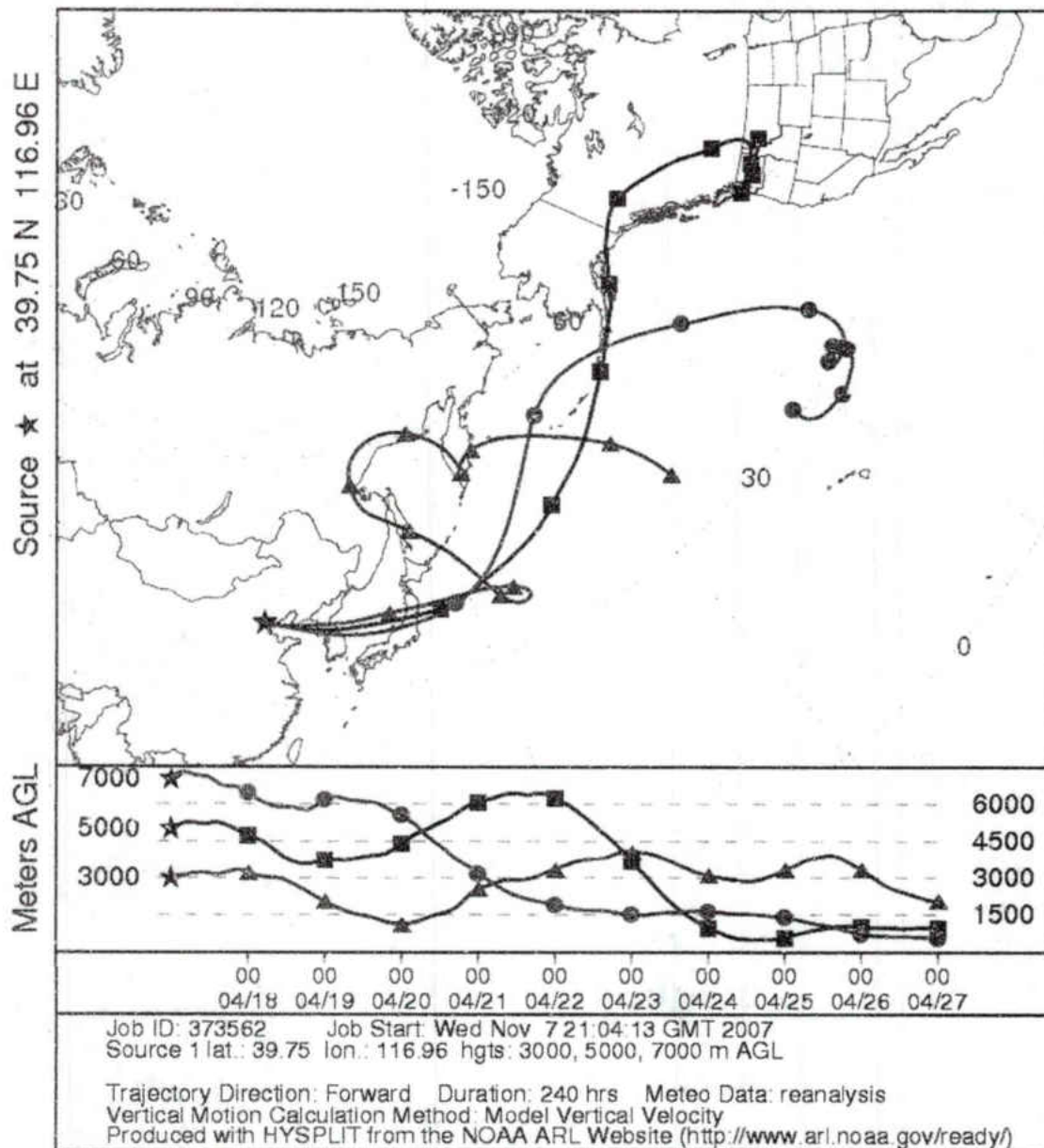


Figure 23. Forward trajectories as computed by the NOAA HYSPLIT model initialized at Xianghe, China on 17 April 2006 at three altitudes: 3000 m, 5000 m, and 7000 m.

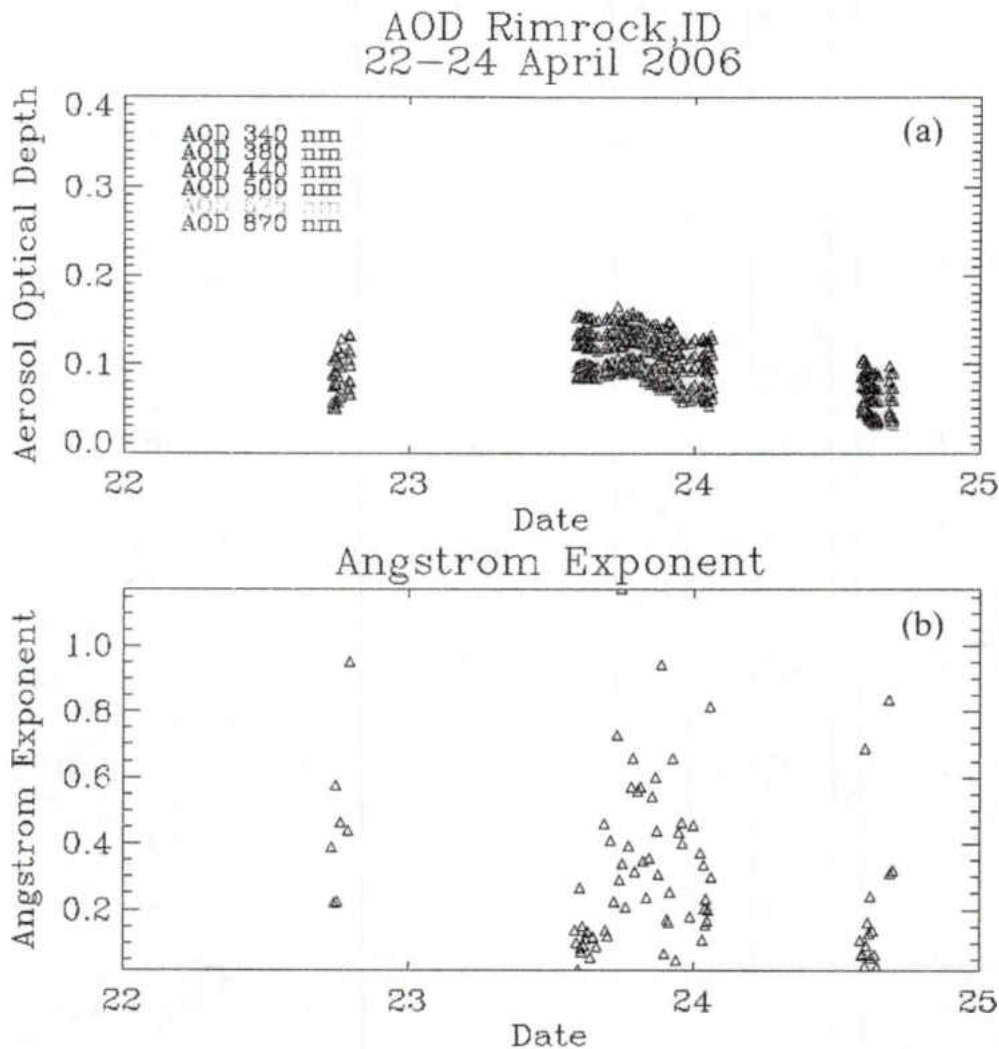


Figure 24. A time series of (a) AOD and (b) Angstrom exponent at Rimrock, ID from 22-25 April.

Weak Dust Event

On 7 April 2006, a low-pressure system moved eastward out of the Gobi Desert with the strongest pressure gradient passing just north of Xianghe (Figure 25b). With this pressure gradient, winds were strong enough to carry dust from the desert to the Pacific while passing over Xianghe. This dust event is clearly viewed from the MODIS visible image in Figure 25a with more aerosol loading around the southeast of Xianghe. The

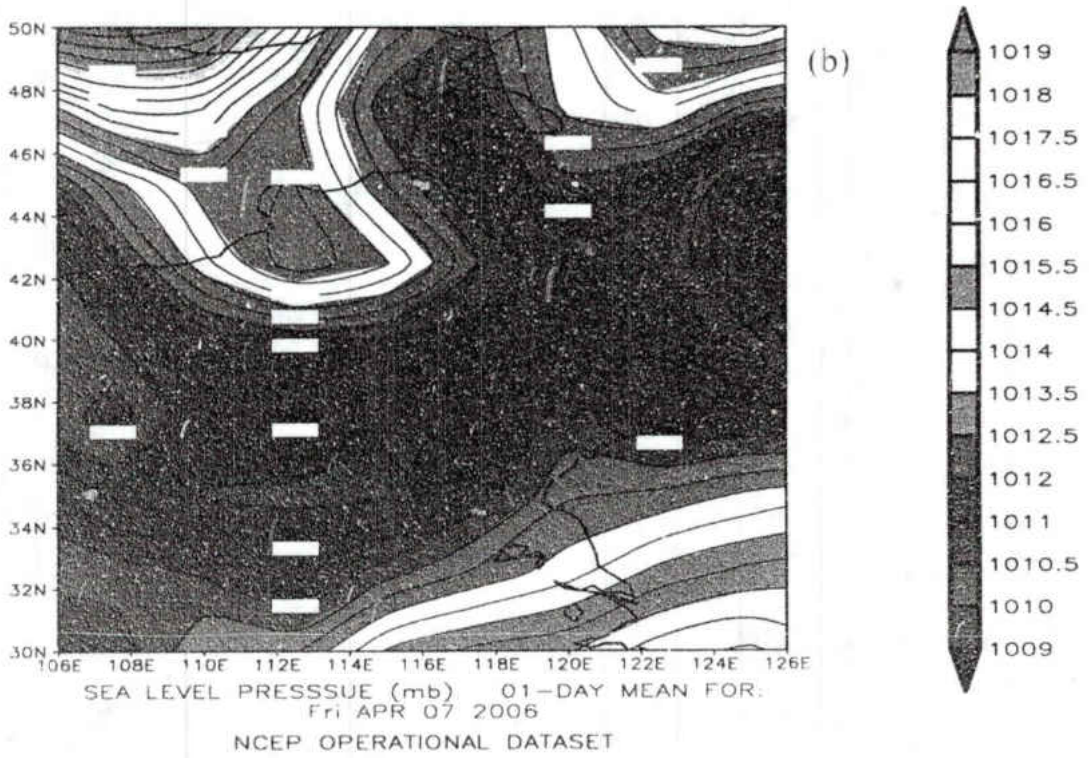


Figure 25. Same as in Figure 10 but for a weak dust event on 7 April 2007.

Bohai Sea can still be seen in the satellite image, indicating that the dust event is not a particularly strong one; whereas in the strong dust event, the Sea could not be seen (Figure 11a).

For the first four hours of the day, the diffuse SW radiation (Figure 26a) was at its highest at over 300 Wm^{-2} , and the direct SW radiation was lower during the peak of the dust storm. The total SW radiation had a maximum of 905 Wm^{-2} . In Figure 26b, AOD is high during the start of the dust event at 1.0 and slowly drops off to 0.5 by the end with a mean of 0.67 at 500 nm. The AE values, however, mirror the variation of AOD, with observations initially very low at 0.1 then slowly rising to 0.3. The sudden jump in direct SW and drop in diffuse SW indicate that the peak of the dust layer had passed the surface site by $\sim 4 \text{ UTC}$.

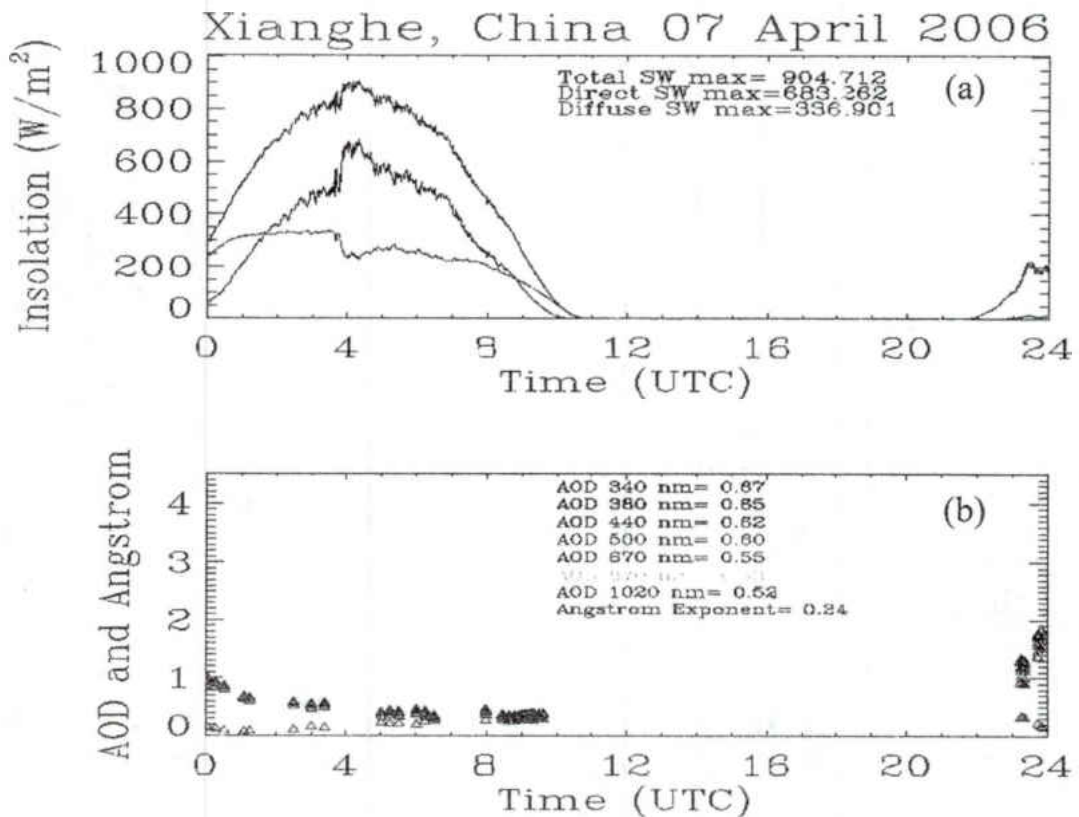


Figure 26. Same as in Figure 8 but for a weak dust event on 7 April 2007.

The mean MODIS AOD over the grid box is 0.8 and TOA albedo is 0.39 (Figure 27). Similar to the strong dust event counterpart, the corresponding TOA albedo is not that high over the southeast of Xianghe. However, the TOA albedo is up to 0.7 over the northeast of Xianghe, which has been identified as clouds from MODIS visible images and has been screened out by the MODIS cloud mask (no aerosol retrievals). MODIS AODs directly over Xianghe associate well with the surface measurements at 0.95. The heaviest dust at the time of the MODIS AOD retrievals are south and east of Xianghe with AOD over 1.0 over the Bohai Sea.

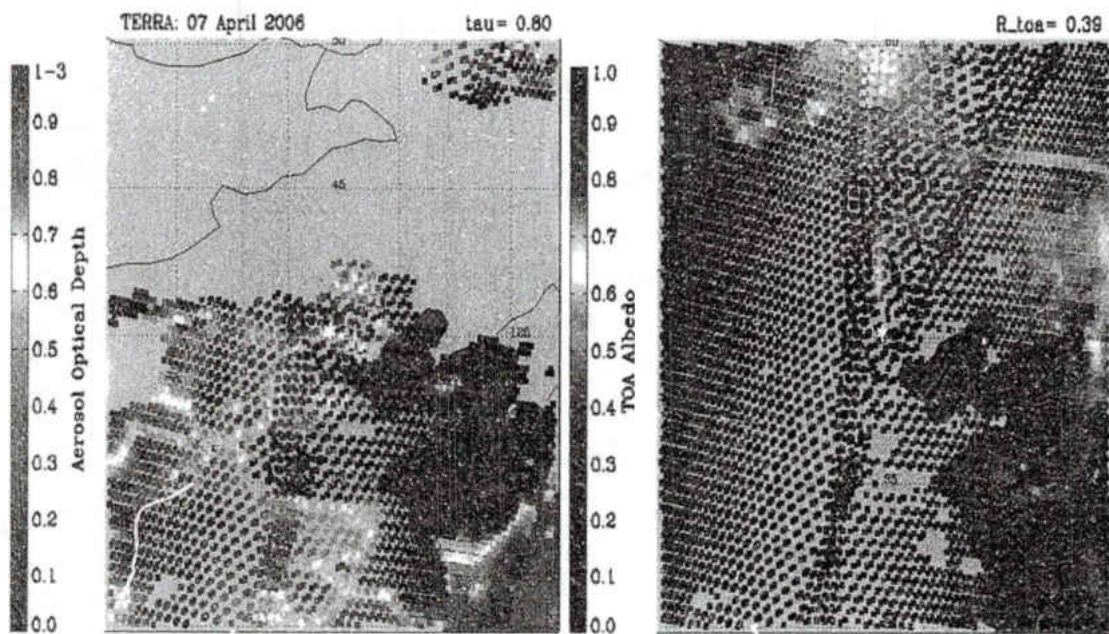


Figure 27. Same as in Figure 9 but for a weak dust event on 7 May 2006.

On 8 April, MODIS AOD was still high at 1.0 as the dust moved from eastern China towards Japan, as seen in Figure 28. The dust moved northeast along Japan following the upper level winds (Figures 29 and 30). The AOD values indicate that the dust tracked with the low-pressure system that continued northeastward to the Pacific but stalled over the west central Pacific due to the blocking high pattern north of the

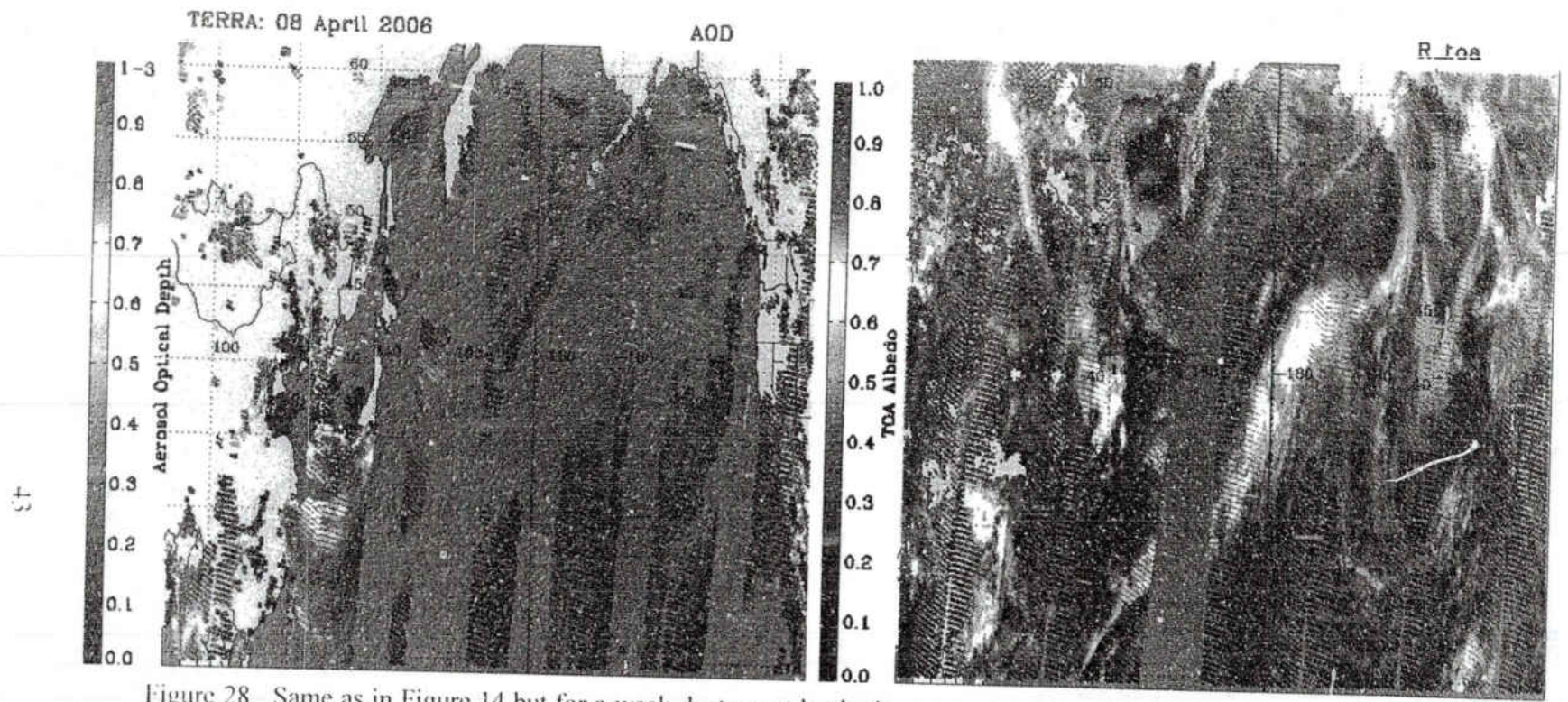


Figure 28. Same as in Figure 14 but for a weak dust event beginning on 7 April 2006. Follow the dust transport from Figures 27-36.

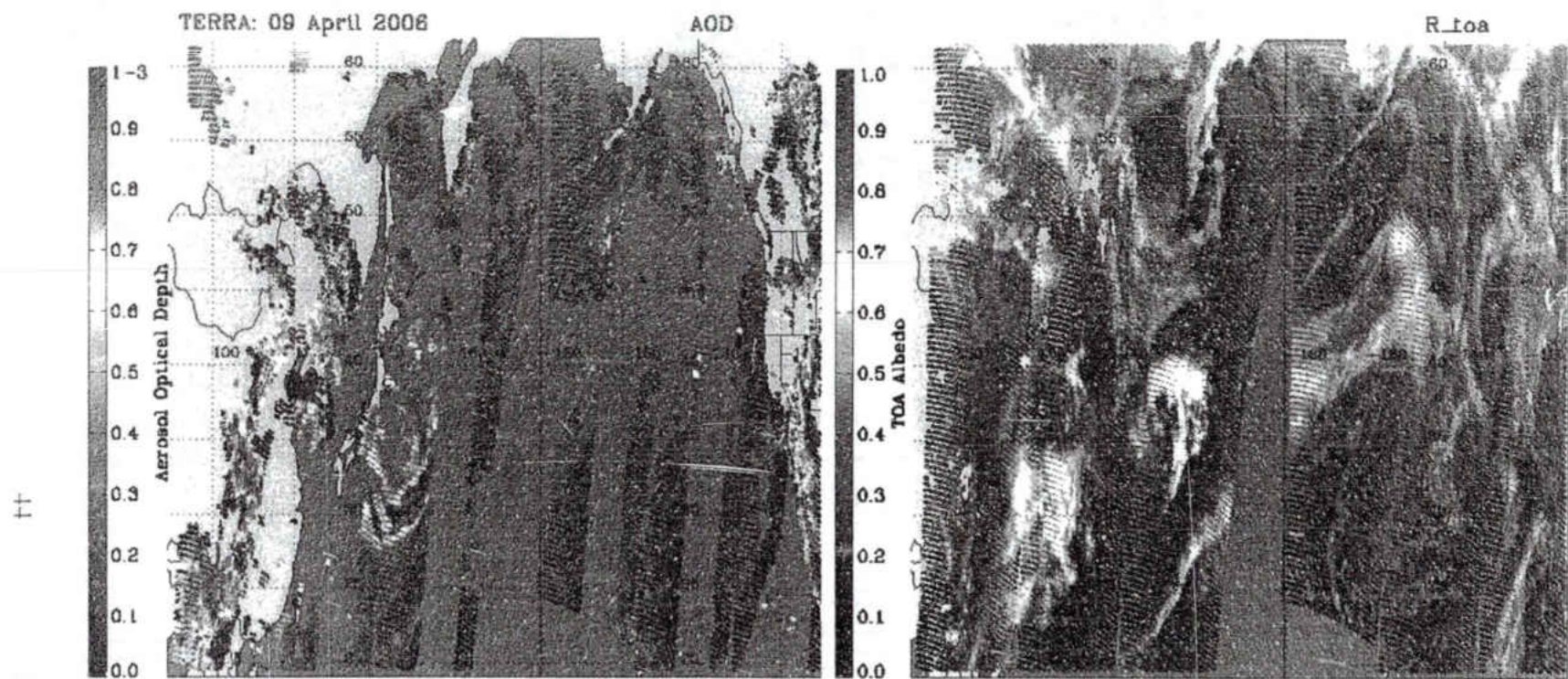


Figure 29. Same as in Figure 28 but for 9 April 2006.

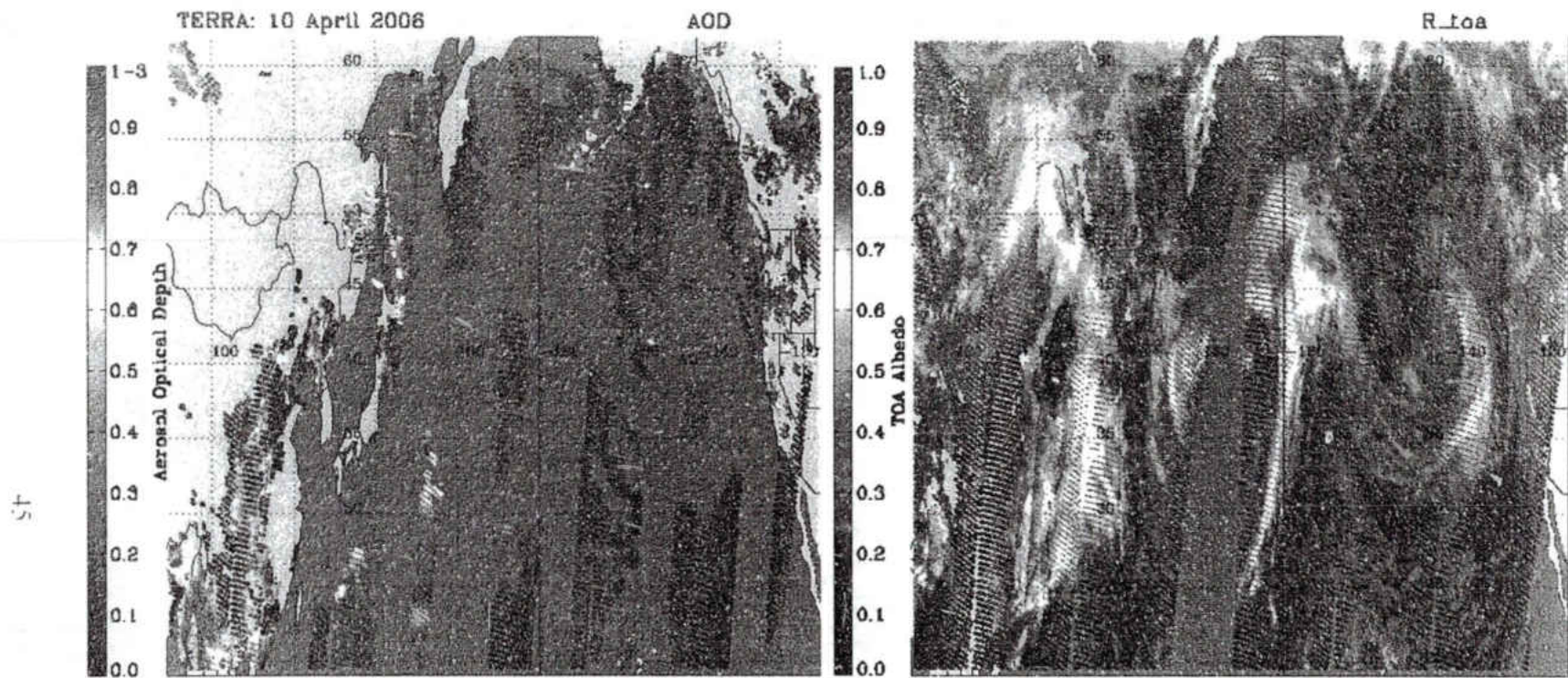


Figure 30. Same as in Figure 28 but for 10 April 2006.

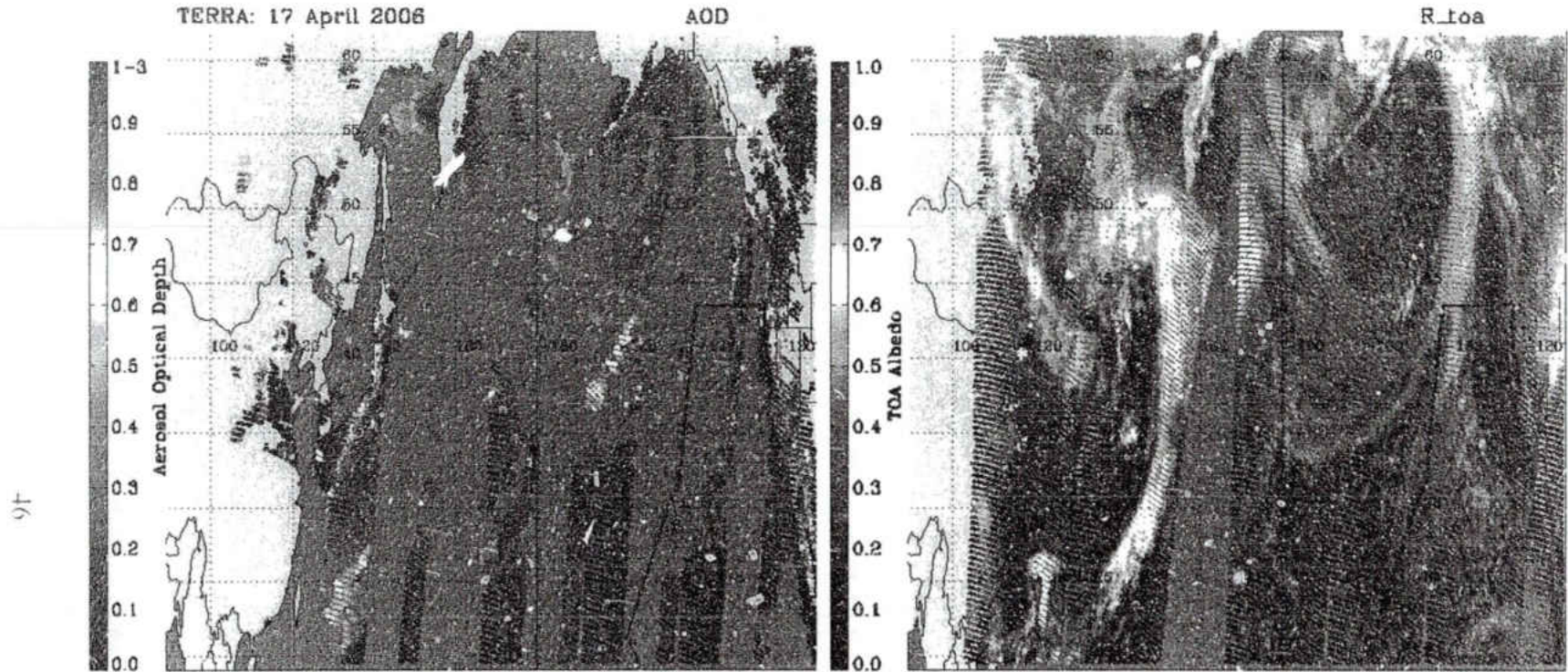


Figure 31. Same as in Figure 28 but for 17 April 2006.

NOAA HYSPLIT MODEL
 Forward trajectories starting at 00 UTC 07 Apr 06
 CDC1 Meteorological Data

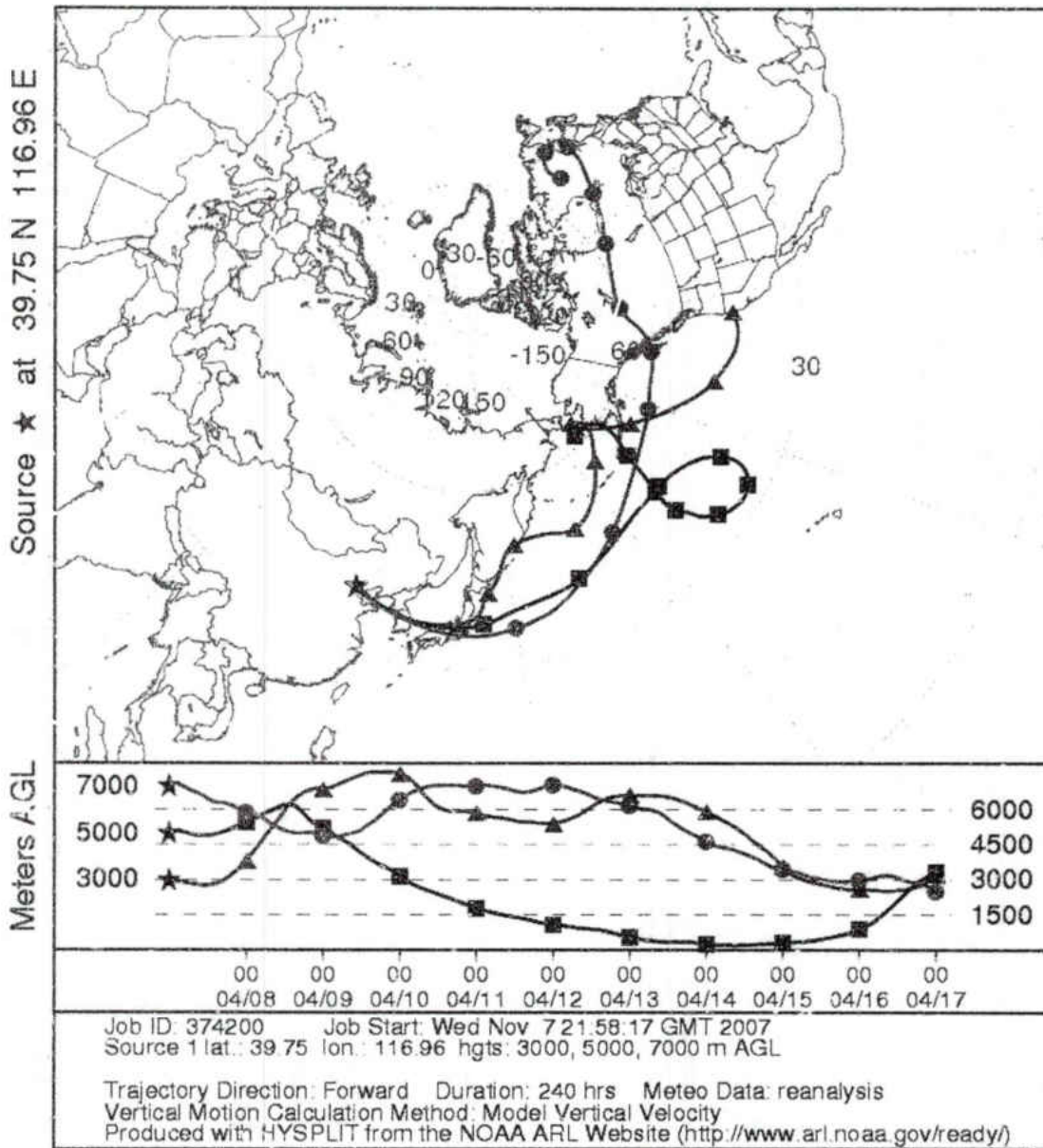


Figure 32. Same as in Figure 23 except initialized on 7 April 2006.

Hawaiian Islands. This slowed the transport of the dust over the Pacific. The dust that was at 3 km (Figure 32) over Xianghe became entrained in this upper blocking pattern for approximately four days until the ridge weakened and the dust resumed its flow south over the eastern Pacific (Figure 31).

The UND/NASA DC-8 aircraft encountered this dust event during 17-18 April 2006 (Figure 33). MODIS AODs on both Terra and Aqua reached a maximum of 0.7 along the flight track where the DIAL (Figure 34) observed the dust layer from 3 to 6 km during the period of 21-23 UTC. The DIAL observations were lower than those of the strong dust event with averaged values of 4.2, 0.5, 80%, and 0.8 for AS-NIR, AS-VIS, Depol., and WD, respectively, during the 9-hr period. The much higher AS-NIR and AS-VIS ratios above 8 km around 20 UTC and 00 UTC have been identified as cirrus clouds from MODIS visible images, and confirmed by GOES-W images (not shown here).

The nephelometer sampled the dust layer twice during the flight. The measurements confirmed the dust at altitudes of 2 and 4 km at 19:30 (Figure 35a) and 23:30 UTC (Figure 35b), respectively. The first profile at 19:30 UTC shows that the dust layer was almost 2 km thick with a maximum scattering coefficient of 40 mm^{-1} , and the second profile shows that the dust was thinner at this time but a higher maximum total scattering of 140 mm^{-1} .

The dust located at 7 km over Xianghe had a much different trajectory than the dust sampled by the DC-8 (at 3-km) and followed the polar jet stream uninhibited to North America in a much shorter time frame. The HYSPLIT model (Figure 32) showed that this dust layer traveled through Canada and reached the northeastern Great Lakes region by 15 April 2006. The AERONET surface site located at Egbert, ON sampled this

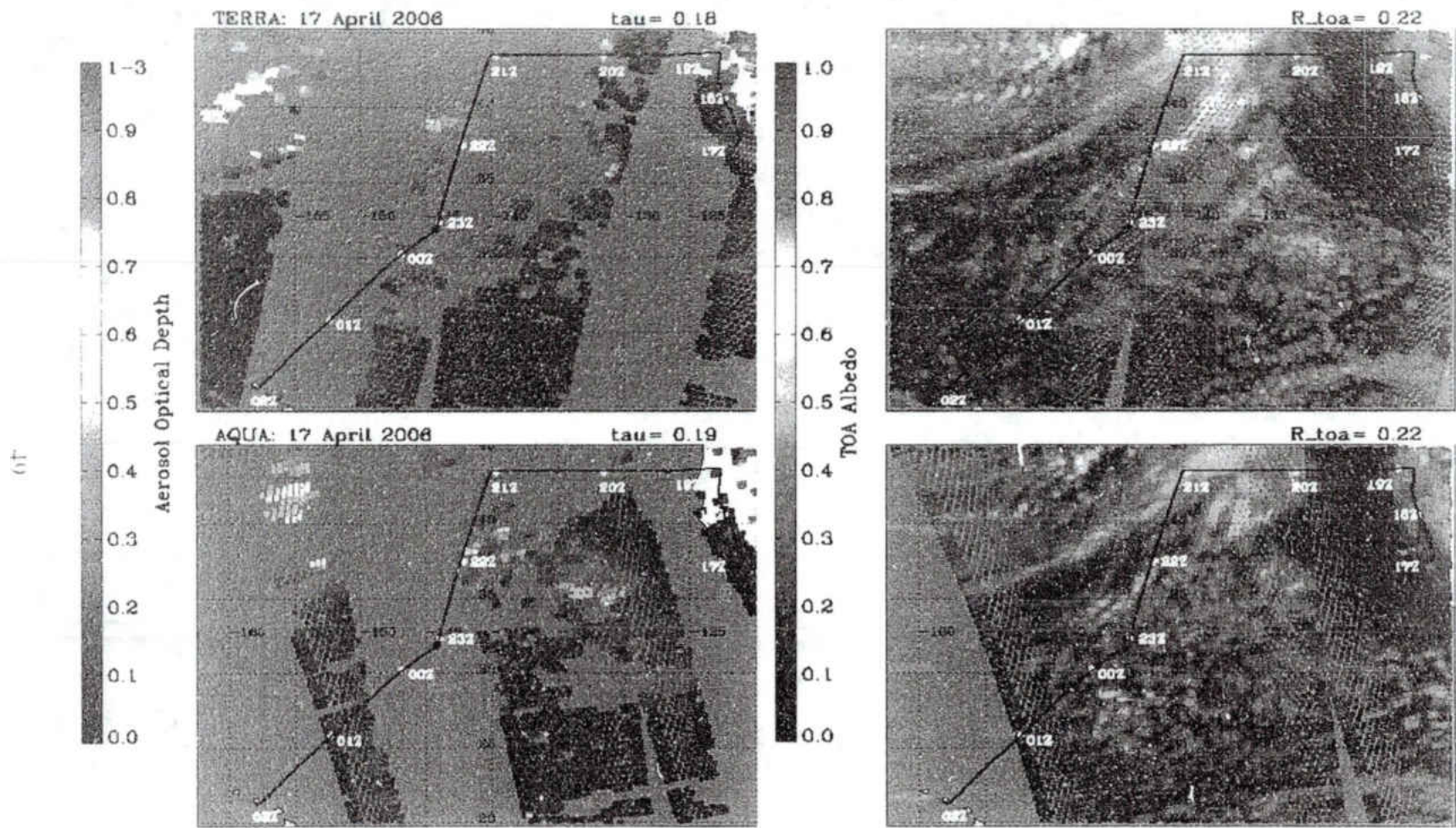


Figure 33. A close-up of the flight track from Figure 36 on 17 April 2006. AOD on the left and TOA albedo from both satellites.

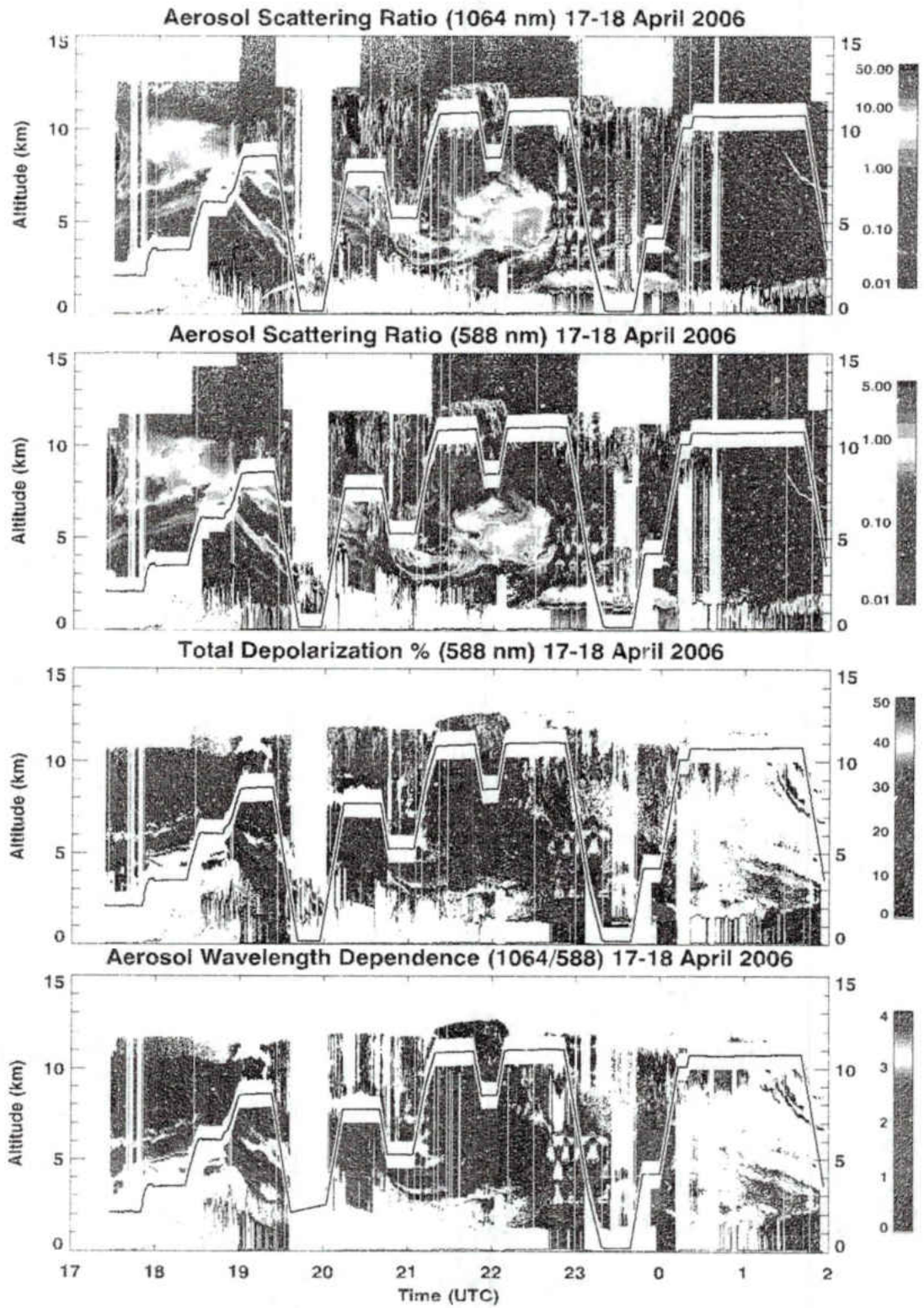


Figure 34. Same as in Figure 21 but for 17-18 April 2006.

Nephelometer Total Scattering (550 nm) Profiles 17 April, 2006

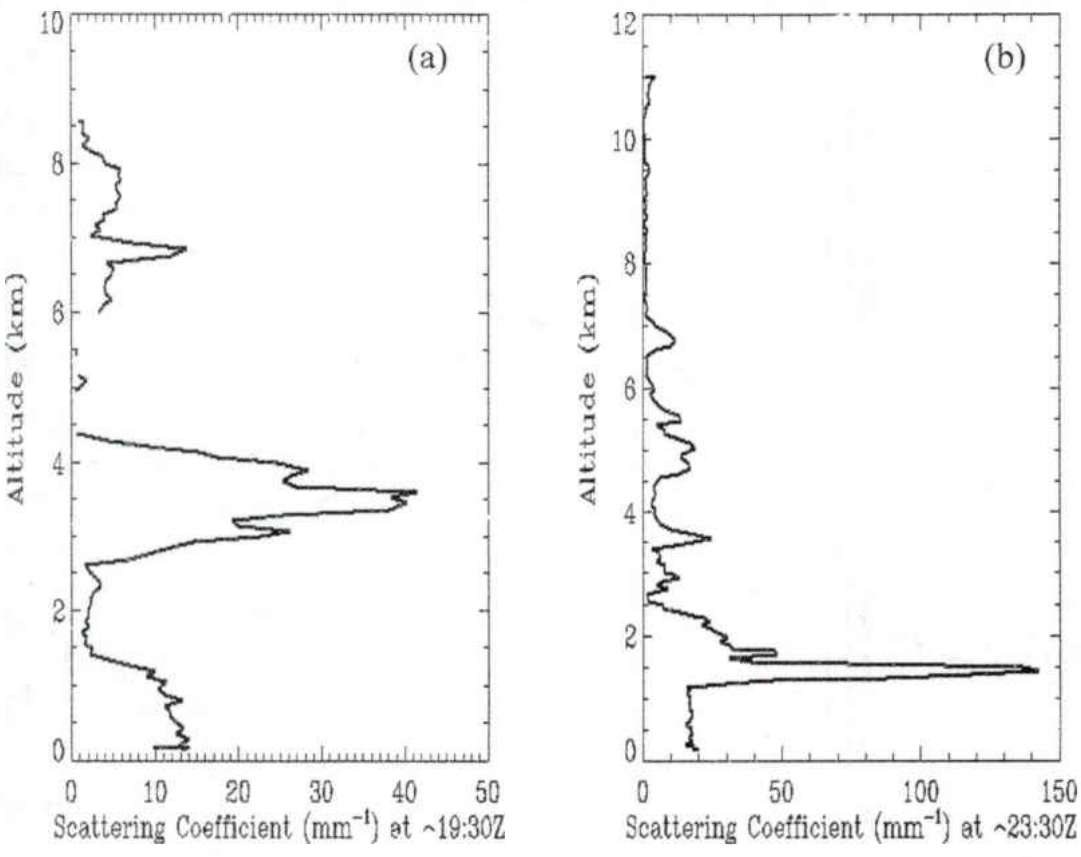


Figure 35. Total scattering coefficients from the nephelometer on the DC-8 on 17 April 2006. The two profile times are at 19:30 (a) and 23:30 (b).

dust event. Figure 36a and b shows a time series of AOD and AE values from 13 to 20 April 2006. The AOD values increase from 0.1 (at 500 nm) on 13 April to above 0.3 on 15-16 April 2006, then slowly decrease to 0.1 on 20 April. The AE values drop dramatically from 1.4 to 0.3 during the period of April 13-15, indicating an influx of relatively large aerosol particles for this event. The Egbert site was able to observe larger values because of the fast track of the dust event in the upper atmosphere from China, whereas the dust layer sampled by the UND/NASA DC-8 aircraft was much older and had more time to settle and disperse over the ocean.

AOD Egbert, ON
13–20 April 2006

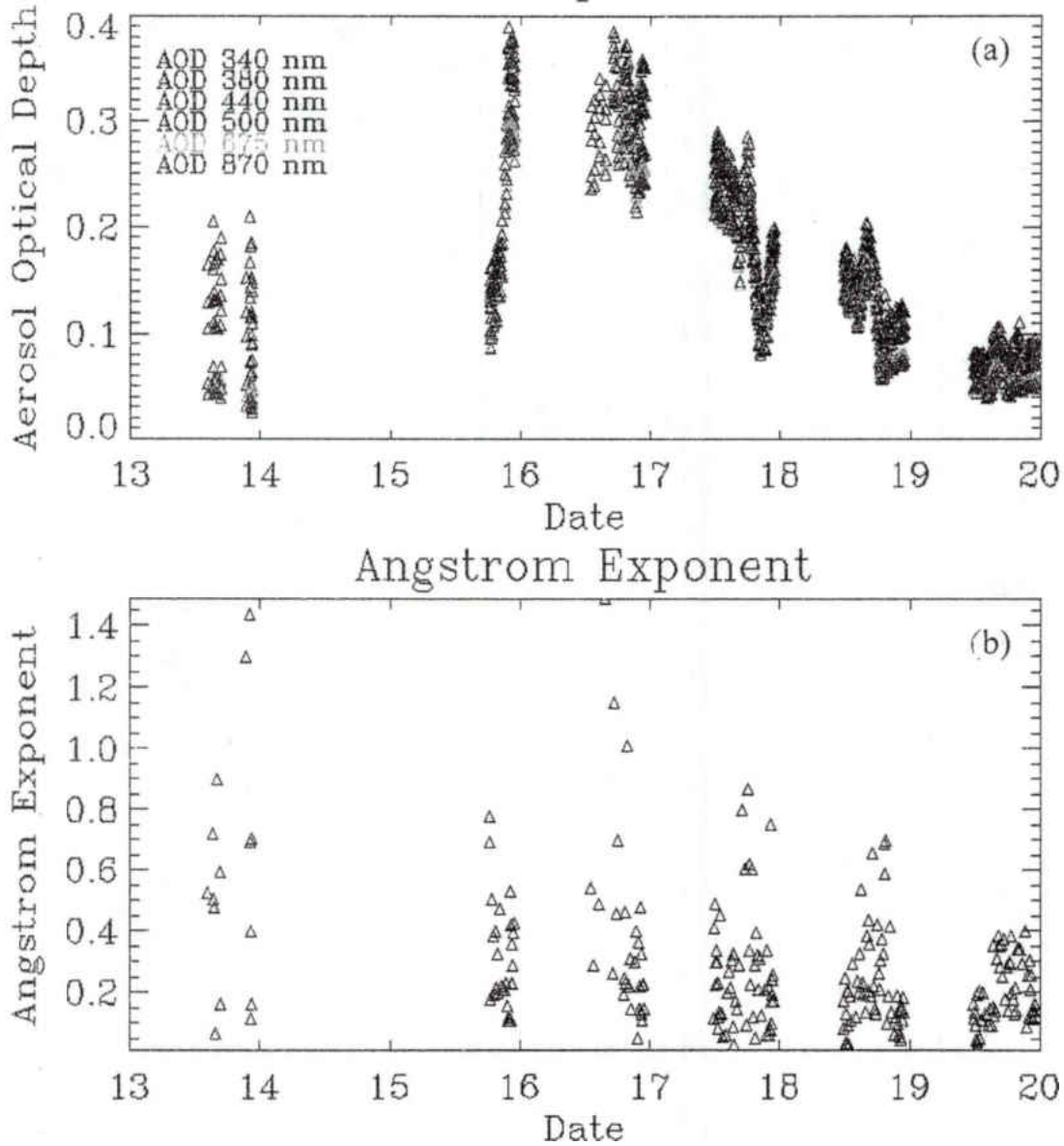


Figure 36. AOD (a) and AE (b) at Egbert, ON during the period from 13 to 20 April 2006. Note the sharp increase in AOD and decrease in AE on 15 April 2006.

CHAPTER IV

DISCUSSION

Table 1 summarizes the measurements and retrievals from surface, satellite, and DC-8 aircraft observations of dust events. These results separate dust events into their source region, the open Pacific Ocean (transport), and sink region based on two clear-sky cases, six strong dust events, and five weak dust events during the April-May 2006 INTEX-B field experiment. The values in the clear-sky (clean, no dust) column provide background values from source to sink, and can be used as a baseline for identifying the dust events originating from East Asia, as well as studying their strength and time evolution during the transpacific transport. Strong and weak dust observations are shown in the last two columns starting with the source (East Asia) and continuing with the transport over the Pacific Ocean. The strong and weak dust events for the sink region are combined into one column due to lack of observations and the loss of some of the dust signal from the Pacific to North America.

Over the source region, the averaged total downwelling SW flux at the surface is 1000 Wm^{-2} during clear-sky conditions, and from that total, 85% of SW flux is direct and 15% is diffuse transmissions. The averaged surface observed/retrieved AOD and AE are 0.25 and 1.27, and the averaged MODIS AOD and CERES TOA albedo are 0.29 and 16.3% under clear-sky conditions. For the strong dust events, their total downwelling SW flux is only 60% of the clear-sky average, and direct and diffuse SW transmissions contribute to 20% and 80% of total SW transmissions, respectively, which is opposite

Table 1. A summary table for the source (Xianghe, China), transport over the Pacific, and sink (North America). The first column lists all the measurements used in the study. The next three columns (clear-sky, strong dust, and weak dust) are averages of all cases used in the study with mean and standard deviation provided, as well as the number of samples in parentheses.

	Measurement	Clear-sky	Strong Dust	Weak Dust
Source	Surface	Xianghe, China		
	Total SW	1000 W/m ²	600 W/m ²	900 W/m ²
	Direct SW	85%	20%	70%
	Diffuse SW	15%	80%	30%
	AOD	0.25 ±0.14(92)	2.0 ±1.34(69)	0.92 ±0.49(122)
	Angstrom Exponent	1.27 ±0.17(92)	0.14 ±0.15(69)	0.36 ±0.19(122)
	Pressure	High	Low	Low
	Satellite			
	AOD	0.29 ±0.11 (11)	1.12 ±0.89 (16)	0.78 ±0.23 (12)
	Albedo	16.34% ±0.87% (11)	24.89% ±9.21% (34)	19.23% ±11.24% (16)
Visible	clear	Strong Yellow appearance	hazy	
Transport	DC-8	Pacific Ocean		
	AS-NIR	0.72 ±0.48	9.58 ±1.07	4.25 ±1.71
	AS-VIS	0.12 ±0.04	1.17 ±0.28	0.40 ±0.17
	Depolarization	7.40% ±3.96%	25.42% ±2.86%	17.52% ±1.69%
	Wavelength Dependence	1.71 ±0.62	0.40 ±0.07	0.75 ±0.14
	Scattering Coefficient	2.99 ±2.44 (16427)	65.77 ±18.45 (255)	25.47 ±8.87 (2980)
	Satellite			
AOD	0.14 ±0.04 (910)	0.34 ±0.14 (188)	0.29 ±0.08 (410)	
		No Dust	Dust	
Sink	Surface	Trinidad Head, CA		
	AOD	0.069 ±0.017(79)	0.142 ±0.028(131)	
	Angstrom Exponent	0.960 ±0.328(79)	0.620 ±0.143(131)	
	Satellite			
	AOD	0.071 ±0.0252(5)	0.125 ±0.0532(16)	
	Surface	Rimrock, ID		
	AOD	0.064 ±0.017(95)	0.121 ±0.034(161)	
	Angstrom Exponent	1.071 ±0.402(95)	0.518 ±0.150(161)	
	Satellite			
	AOD	0.148 ±0.0663(21)	0.27 ±0.213(9)	
	Surface	Egbert, ON Canada		
	AOD	0.087 ±0.053(186)	0.202 ±0.083(170)	
Angstrom Exponent	1.283 ±0.190(186)	0.344 ±0.111(170)		
Satellite				
AOD	0.132 ±0.190(22)	0.181 ±0.022(6)		

to the clear-sky results. Their averaged AOD (~2) and averaged AE (0.14) are higher and lower, respectively, than their clear-sky counterparts. The satellite retrieved AOD and TOA albedo are 1.12 and 25%, consistent with the surface observations. For the weak dust events, their averaged values fall between the clear-sky and strong dust results. For example, their averaged total downwelling SW flux is 90% of the clear-sky mean value; the mean AOD is around 0.78-0.92, the mean AE is 0.36, and the TOA albedo is 19%.

Over the eastern Pacific Ocean, the averaged AS-NIR, AS-VIS, Depol., WD, scattering coefficient, and MODIS AOD are 0.72, 0.12, 7.4%, 1.71, 3.0, 0.14, respectively, during the clear-sky periods. For the strong dust events, however, their averages increase significantly, except for WD, with corresponding values of 9.58, 1.17, 25.4%, 0.4, 65.8, and 0.34. The averages for weak dust events are very similar to the results in their source region and fall between clear-sky and strong dust observations/retrievals.

Over the sink region, only averages for clear-sky (no dust) and dust events from three surface sites are provided. There are two reasons for choosing these three sites: (1) they are located within the dust sink region as tracked by the forward trajectories, and (2) their observations are quality controlled. Compared to the clear-sky AOD values over their source region, the AOD values over North America are much smaller (0.07 vs. 0.25). This result suggests that aerosol loading over North America is much lower than over East Asia, and that the atmosphere is cleaner during clear-sky periods. Although the averaged AOD and AE values for dust events are lower than the clear-sky values over their source region (East Asia), AODs are higher and AEs are lower than their clear-sky background values.

Clear-sky values over the Asian dust source, open Pacific, and sink regions are presented because they represent different backgrounds. In turn, they provide different baselines for one to analyze the dust strength and evolution. The averages in Table 1 may help climate modelers improve Asian dust simulations and understand its impact on regional and global climate changes.

CHAPTER V

CONCLUSIONS

Several data sets have been used to analyze the Asian dust events during the April-May 2006 INTEX-B field experiment, including surface AOD, solar irradiance, and Angström exponent from EAST-AIRE over China, and AERONET over North America. The satellite AOD and TOA albedo are derived from MODIS and CERES observations on both Terra and Aqua platforms. The DIAL and nephelometer measurements on the UND/NASA DC-8 aircraft are also used in this study. The approach for analyzing this integrated dataset is as follows. First, clear-sky (clean, no dust) events based on surface and satellite observations from source to sink regions were selected. Second, these clear-sky values were used as a background to select strong and weak dust events in their source region, and then track them using both MODIS/CERES retrievals and the forward trajectory model. The physical and optical properties of the strong and weak dust events selected in this study are summarized below:

- 1) A significant Asian dust storm occurred on 17 April 2006 driven by a strong low-pressure system that swept over Mongolia, the Gobi Desert, and then over Xianghe. The observed total downwelling SW flux over Xianghe was only 46% of the clear-sky value, with almost no direct transmission, and with downwelling diffuse SW surface fluxes nearly double the clear-sky values. The surface averaged AOD increased from 0.17 (clear-sky) to 4.0, and the AE dropped from 1.26 (clear-sky) to below 0.1. The MODIS AOD was consistent with these

surface results. When this dust event travelled across the Pacific Ocean, its strength degraded due to dispersion and larger particles settling out, as reflected in lower AOD values over the Pacific Ocean and North America. The UND/NASA DC-8 aircraft observed this dust event over the eastern Pacific Ocean on 23-24 April 2006 with much higher aerosol scattering ratios of 10.5 at 1064 nm and 2.0 at 588 nm and a depolarization of 25%. The DC-8 nephelometer also observed this dust event in-situ and confirmed that the highest scattering coefficients ranged from 80-100 mm^{-1} .

2) The formation and dissipation processes and characteristics of the weak dust event were similar to its strong dust counterpart, but its aerosol loading and strength was much weaker. Most of the physical and optical properties for the weak dust event fell between the clear-sky and strong dust observations.

3) A forward trajectory model (HYSPLIT) was used to track the dust events from their source region over Pacific Ocean to its sink region. The dust layers at different altitudes over the source region can have drastically different trajectories and time evolutions when or if they arrive to North America. In general, the dust events originating from East Asia reached North America in about a week, which is consistent with the findings from other studies.

These results provide invaluable information for quantifying the physical and optical properties of Asian dust as well as their strength and evolution from their source to sink regions. In the future, it is necessary to use this integrated dataset to investigate the impact of these dust events on regional and global climates and to analyze the composition of any pollution that was carried by these dust clouds from China.

Eventually, these studies will help climate modelers obtain more accurate climate predications. The use of aircraft data in this study proved particularly useful in understanding the spatio-temporal extent of Asian dust downstream of its source and/or validated the satellite observations of aerosol optical properties in both the source/sink regions and transport processes. The analysis in this study, particular for DC-8 DIAL, will be valuable for us to analyze the recently launched CALIPSO (Cloud-Aerosol Lidar and Infrared Pathfinder Satellite Observations) retrieved aerosol properties in the future. As the number of Asian dust storms increases and with no sign of industrial China reducing its anthropogenic contribution, future field campaigns studying intercontinental aerosol transport are necessary in order to continue our understanding of the impact of aerosols on downwind regions like North America.

REFERENCES

- Ackerman, S., K. Strabala, P. Menzel, R. Frey, C. Moeller, and L. Gumley (1998), Discriminating clear sky from clouds with MODIS, *J. Geophys. Res.*, *103*, 32 139-32 140.
- Anderson, T. L., and J. A. Ogren (1998), Determining Aerosol Radiative Properties Using the TSI 3563 Integrating Nephelometer, *Aero. Sci. Tech.*, *29*, 57-69.
- Angström, A. (1929), On the atmospheric transmission of sun radiation and on dust in the air, *Geograph. Ann.*, *11*, 156-166.
- Bachmeier, A. S., R. E. Newel, M. C. Shipham, Y. Zhu, D. R. Blake, and E. V. Browell (1996), PEM-West A: Meteorological overview, *J. Geophys. Res.*, *101*(D1), 1655-1677.
- Browell, E.V., S. Ismail, and W. B. Grant (1998), Differential absorption lidar (DIAL) measurements from air and space, *Appl. Phys. B*, *67*, 399-410.
- Burdakov, A. S. and S. B. Pole (1984), Influence of human activity on the natural plague focus in the central Asian desert, *Sov. J. Ecol.*, *15*(3), 142-145.
- Chambers, L.H., B. Lin, and D.F. Young (2002), Examination of new CERES data for evidence of tropical Iris feedback, *J. Clim.*, *15*, 3719-3726.
- Chin, M., T. Diehl, P. Ginoux, and W. Malm (2007), Intercontinental transport of pollution and dust aerosols: Implications for regional air quality, *Atmos. Chem. Phys.*, *7*, 5504-5517.

- DeMott, P. J., K. Sassen, M. R. Poellot, D. Baumgardner, D. C. Rogers, S. D. Brooks, A. J. Prenni, and S. M. Kreidenweis (2003), African dust aerosols as atmospheric ice nuclei, *Geophys. Res. Lett.*, *30*(14), 1732, doi:10.1029/2003GL017410.
- Draxler, R.R. and G.D. Rolph (2003), HYSPLIT (HYbrid Single-Particle Lagrangian Integrated Trajectory) Model access via NOAA ARL READY Website [<http://www.arl.noaa.gov/ready/hysplit4.html>], NOAA Air Resources Laboratory, Silver Spring, MD.
- Duce, R. A., C. K. Unni, B. J. Ray, J. M. Prospero, and J. T. Merrill (1980), Long-Range Atmospheric Transport of Soil Dust from Asia to the Tropical North Pacific: Temporal Variability, *Science*, *209*, 4464, doi:10.1126/science.209.4464.1522.
- Eck, T. F., B. N. Holben, J. S. Reid, O. Dubovik, A. Smirnov, N. T. O'Neill, I. Slutsker, and S. Kinne (1999), Wavelength dependence of the optical depth of biomass burning, urban, and desert dust aerosols, *J. Geophys. Res.*, *104*(D24), doi:10.1029/1999JD900923.
- Eckhardt, S., A. Stohl, H. Wernli, P. James, C. Forster, and N. Spichtinger (2004), A 15-Year Climatology of Warm Conveyor Belts, *J. Climate*, *17*, 218-237.
- Gillette, D. (1978), A wind tunnel simulation of the erosion of soil: Effect of soil texture, sand-blasting, wind speed, and soil consolidation on the dust production, *Atmos. Environ.*, *12*, 1735-1743.
- Gueymard C., C. Laulainen, J. Vaughan, and F. Vignola (2000), China's dust affects solar resource in the U.S.: A case study. *Solar 2000: Proc. ASES Annual Conf.*, Madison, WI, U.S. Department of Energy, 383-389.

- Holben, B. N., T. F. Eck, I. Slutsker, D. Tanré, J. P. Buis, A. Setzer, E. Vermote, J. A. Reagan, Y. J. Kaufman, T. Nakajima, F. Lavenu, I. Jankowiak, and A. Smirnov (1998), AERONET-A federated instrument network and data archive for aerosol characterization, *Remote Sens. Environ.*, *66*, 1-16.
- Huang, J., P. Minnis, B. Lin, T. Wang, Y. Yi, Y. Hu, S. Sun-Mack, and K. Ayers (2006), Possible influences of Asian dust aerosols on cloud properties and radiative forcing observed from MODIS and CERES, *Geophys. Res. Lett.*, *33*, L06824, doi:10.1029/2005GL024724.
- Huebert, B. J., T. Bates, P. B. Russel, G. Shi., Y. J. Kim, K. Kawamura, G. Carmichael, and T. Nakajima (2003), An overview of ACE-Asia: Strategies for quantifying the relationships between Asian aerosols and their climatic impacts, *J. Geophys. Res.*, *108*(D23), 8633 doi:10.1029/2003JD003550.
- Husar, R. B., D. M. Tratt, B. A. Schichtel, S. R. Falke, F. Li, D. Jaffe, S. Gassó, T. Gill, N. S. Laulainen, F. Lu, M. C. Reheis, Y. Chun, D. Westphal, B. N. Holben, C. Gueymard, I. McKendry, N. Kuring, G. C. Feldman, C. McClain, R. J. Frouin, J. Merrill, D. DuBois, F. Vignola, T. Murayama, S. Nickovic, W. E. Wilson, k. Sassen, N. Sugimoto, and W. C. Malm (2001), Asian dust events of April 1998, *J. Geophys. Res.*, *106*(D16), 18 317-18 330.
- Ignatov, A., P. Minnis, N. Loeb, B. Wielicki, W. Miller, S. Sun-Mack, D. Tanré, L. Remer, I. Laszlo, and E. Geier (2005), Two MODIS Aerosol Products over Ocean on the *Terra* and *Aqua* CERES SSF Datasets, *J. Atmos. Sci.*, *62*, 1008-1031.

- Intergovernmental Panel on Climate Change (2001), *Climate Change 2001: The Scientific Basis. Contribution of Working Group I to the Third Assessment Report of the Intergovernmental Panel on Climate Change*, edited by J. T. Houghton et al., Cambridge Univ. Press, New York, 881 pp.
- Intergovernmental Panel on Climate Change (2007), *Climate Change 2007: The Physical Science Basis. Contribution of Working Group I to the Fourth Assessment Report of the Intergovernmental Panel on Climate Change*, edited by S. Solomon et al., Cambridge Univ. Press, New York, 996 pp.
- Jacob, D. J., J. H. Crawford, M. M. Kleb, V. S. Connors, R. J. Bendura, J. L. Raper, G. W. Sachse, J. C. Gille, L. Emmons, and C. L. Heald (2003), Transport and Chemical Evolution over the Pacific (TRACE-P) aircraft mission: Design, execution, and first results, *J. Geophys. Res.*, *108*(D20), 9000, doi:10.1029/2002JD003276.
- Jaffe, D., I. McKendry, T. Anderson, and H. Price (2003a), Six 'new' episodes of trans-pacific transport of air pollutants, *Atmos. Environ.*, *37*, 391-404.
- Jaffe, D., J. Snow, and O. Cooper (2003b), The 2001 Asian Dust Events: Transport and Impact on Surface Aerosol Concentrations in the U.S., *Eos Trans. AGU*, *84*(46), 501-516.
- Levin, Z., and E. Ganor (1996), The effects of desert particles on cloud and rain formation in the eastern Mediterranean, in *The Impact of Desert Dust Across the Mediterranean*, edited by S. Guerzoni and R. Chester, pp. 77-86, Kluwer Acad., Norwell, Mass.

- Li, Z., X. Xia, M. Cribb, W. Mi, B. Holben, P. Wang, H. Chen, S.-C. Tsay, T. Eck, F. Zhao, E. Dutton, and R. Dickerson (2007), Aerosol optical properties and its radiative effects in Northern China, *J. Geophys. Res.*, *112*, D22S01, doi:10.1029/2006JD007382.
- Li, Z., T. Yuan, M. Cribb, and C. Li (2008), East Asian Study of Tropospheric Aerosols: an International Regional Experiment (EAST-AIRE), [http://www.atmos.umd.edu/~yuan/web_proj/station.htm].
- Loeb, N. G., N. Manalo-Smith, S. Kato, W. F. Miller, S. K. Gupta, P. Minnis, and B. A. Wielicki (2003), Angular distribution models for top-of-atmosphere radiative flux estimation from CERES instrument on the TRMM satellite, Part I: Methodology, *J. Appl. Meteor.*, *42*, 240-265.
- Martins, J., Didier Tanré, L. Remer, Y. Kaufman, S. Mattoo, and R. Levy (2002), MODIS cloud screening for remote sensing of aerosols over oceans using spatial variability, *Geophys. Res. Lett.*, *29*, 8009, doi:10.1029/2001GL013252.
- Matthews, G., K. Priestley, P. Spence, D. Cooper and D. Walikainen (2005), Compensation for spectral darkening of short wave optics occurring on the Cloud's and the Earth's Radiant Energy System, Earth Observing Systems X (Proc. SPIE), 588212.
- Murayama, T., N. Sugimoto, I. Uno, K. Kinoshita, K. Aoki, N. Hagiwara, Z. Liu, I. Matsui, T. Sakai, T. Shibata, K. Arao, B.-J. Sohn, J.-G. Won, S.-C. Yoon, T. Li, J. Zhou, H. Hu, M. Abo, K. Iokibe, R. Koga, and Y. Iwasaka (2001), Ground-based network observation of Asian dust events of April 1998 in east Asia, *J. Geophys. Res.*, *106*(D16), 18 345-18 359.

- Parrington, J. R., W. H. Zoller, and N. K. Aras (1983), Asian dust: Seasonal transport to the Hawaiian Islands, *Science*, *220*, 195-197.
- Parrish, D. D., Y. Kondo, O. R. Cooper, C. A. Brock, D. A. Jaffe, M. Trainer, T. Ogawa, G. Hübler, and F. C. Fehsenfeld (2004), Intercontinental Transport and Chemical Transformation 2002 (ITCT 2K2) and Pacific Exploration of Asian Continental Emission (PEACE) experiments: An overview of the 2002 winter and spring intensives, *J. Geophys. Res.*, *109*, D23S01, doi:10.1029/2004JD004980.
- Prospero, J. M. (1999), Long-range transport of mineral dust in the global atmosphere: Impact of African dust on the environment of the southeastern United States, *Proc. Natl. Acad. Sci.*, *96*, 3396-3403.
- Qiu, J. H., and J. Sun (1994), Optical remote sensing of the dust storm and the analysis, *Chin. J. Atmos. Sci.*, *18*, 1-10.
- Remer, L., Y. Kaufman, D. Tanré, S. Mattoo, S. Chu, J. Martins, R.-R. Li, C. Ichoku, R. Levy, R. Kleidman, T. Eck, E. Vermote, and B. Holben (2005), The MODIS aerosols algorithm, products, and validation, *J. Atmos. Sci.*, *62*, 947-973.
- Rosenfeld, D., Y. Rudich, and R. Lahav (2001), Desert dust suppressing precipitation: A possible desertification feedback loop, *Proc. Natl. Acad. Sci.*, *98*, 11, 5675-5980.
- Roskovensky, J. K. and K. N. Liou (2005), Differentiating airborne dust from cirrus clouds using MODIS data, *Geophys. Res. Lett.*, *32*, L12809, doi:10.1029/2005GL022798.
- Shaw, G.E. (1980), Transport of Asian desert aerosol to the Hawaiian Islands, *J. Appl. Meteorol.*, *19*, 1254-1259.

- Singh, H. B., W. H. Brune, J. H. Crawford, H. Fuelberg, and D. J. Jacob (2005), The Intercontinental Chemical Transport Experiment – Phase B (INTEX-B): An update, Retrieved October 5, 2006, from NASA LaRC website: [http://cloud1.arc.nasa.gov/docs/intex-na/INTEX-B_White_Paper.pdf].
- Sun, J., M. Zhang, and T. Liu (2001), Spatial and temporal characteristics of dust storms in China and its surrounding regions, 1960-1999: Relations to source area and climate, *J. Geophys. Res.*, *106*, 10 325-10 333.
- Szykman, J., D. Mintz, J. Creilson, and M. Wayland (2003), Impact of April 2001 Asian Dust Event on Particulate Matter Concentrations in the United States, *Nat. Air Qual. Emis. Trends Rep.-Special Studies*, S1-S12, EPA.
- Tanré, D., Y. Kaufman, M. Herman, and S. Matoo (1997), Remote sensing of aerosol properties over oceans using the MODIS/EOS spectral radiances, *J. Geophys. Res.*, *102*(D14), 16 971-16 988.
- Tanré, D., Y. J. Kaufman, B. N. Holben, B. Chatenet, A. Karnieli, F. Lavenu, L. Blarel, O. Dubovik, L. A. Remer, and A. Smirnov (2001), Climatology of dust aerosol size distribution and optical properties derived from remotely sensed data in the solar spectrum, *J. Geophys. Res.*, *106*(D16) 18 205-18 217.
- Tratt, D. M., R. J. Frouin, and D. L. Westphal (2001), April 1998 Asian dust event: A southern California perspective, *J. Geophys. Res.*, *106*(D16), 18 371-18 379.
- Uematsu, M, R. A. Duce, J. M. Prospero, L. Chen, J. T. Merrill, and R. L. McDonald (1983), Transport of mineral aerosol from Asia over the North Pacific Ocean, *J. Geophys. Res.*, *88*(C9), 5343-5352.

- VanCuren, R. A., and T. A. Cahill (2002), Asian aerosol in North America: Frequency and concentration of fine dust, *J. Geophys. Res.*, *107*, 4804, doi:10.1029/2002JD002204.
- Wielicki, B. A., B. R. Barkstrom, E. F. Harrison, R. B. Lee III, G. L. Smith, and J. E. Cooper (1996), Clouds and the Earth's Radiant Energy System (CERES): An Earth Observing System Experiment, *Bull. Amer. Meteor. Soc.*, *77*, 853-868.
- Xia, X., H. Chen, Z. Li, P. Wang, and J. Wang (2007), Significant reduction of surface solar irradiance induced by aerosols in a suburban region in northeastern China, *J. Geophys. Res.*, *112*, D22S02, doi:10.1029/2006JD007562.